NASA CR-135203
TRW ER-7930

(NASA-CR-135203) COST ANALYSIS OF ADVANCED TURBINE BLADE MANUFACTURING PROCESSES Final Report, Oct. 1976 - April 1977 (TRW, Inc., Cleveland, Ohio.) 89 p HC A05/MF A01 CSCL 21E G3/07

N78-10092

Unclas 50099

COST ANALYSIS OF ADVANCED TURBINE BLADE MANUFACTURING PROCESSES

FINAL REPORT

prepared for

NATIONAL AERONAUTICS AND SPACE ADMINISTRATION

NASA Lewis Research Center

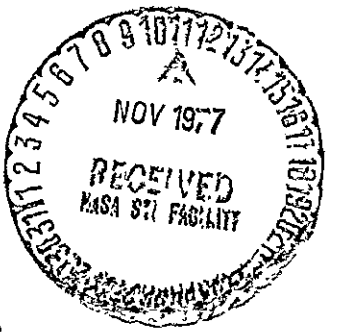

Contract NAS 3-20378

N. T. SAUNDERS, Project Manager

N78-10092

1. Report No	2. Government Accession No.	3. Recipient's Catalog No.
NASA CR-135203		

4. Title and Subtitle	5. Report Date
Cost Analysis of Advanced Turbine Blade Manufacturing Processes	October, 1977
	6. Performing Organization Code

7. Author(s)	8. Performing Organization Report No.
C. F. Barth D. E. Blake T. S. Stelson	ER-7930
	10. Work Unit No.

9. Performing Organization Name and Address	11. Contract or Grant No.
TRW Inc. 23555 Euclid Avenue Cleveland, Ohio 44117	NAS-3-20378

12. Sponsoring Agency Name and Address	13. Type of Report and Period Covered
National Aeronautics and Space Administration Washington, D.C. 20546	Final Report October 1976 - April 1977
	14. Sponsoring Agency Code

15. Supplementary Notes
Project Manager, N. T. Saunders
NASA-Lewis Research Center
21000 Brookpark, Cleveland, Ohio 44117

16. Abstract

A rigorous analysis was conducted to estimate relative manufacturing costs for high technology gas turbine blades prepared by three candidate materials/process systems. The manufacturing costs for the same turbine blade configuration of directionally solidified eutectic alloy (DSE), an oxide dispersion strengthened superalloy (ODSS), and a fiber reinforced superalloy (FRS) were compared on a relative basis to the costs of the same blade currently in production utilizing the directional solidification (DS) process. An analytical process cost model was developed to quantitatively perform the cost comparisons. The impact of individual process yield factors on costs were also assessed as well as effects of process parameters, raw materials, labor rates and consumable items.

17. Key Words (Suggested by Author(s))	18. Distribution Statement
Cost Analysis High Technology Turbine Blading Manufacturing Analyses Process Modeling	Unclassified - Unlimited

19. Security Classif. (of this report)	20. Security Classif. (of this page)	21. No. of Pages	22. Price*
Unclassified	Unclassified		

* For sale by the National Technical Information Service, Springfield, Virginia 22151

FOREWORD

This program was conducted by the Materials Technology Laboratories under Contract Number NAS-3-20378 for the Lewis Research Center of the National Aeronautics and Space Administration. The program manager was Dr. C. F. Barth with technical support provided by Dr. T. S. Piwonka, D.S. and D.S.E. systems; Mr. W. D. Brentnall, F.R.S. systems; Mr. C. R. Cook and Mr. D. J. Moracz, O.D.S.S. systems; Mr. D. E. Blake, Process Analysis; and Mr. T. S. Stelson, Cost Models. The bulk of this work was conducted within the Materials Development Department, Dr. I. J. Toth, Manager, and has been assigned the TRW internal project number 512-002645-22.

T. S. Piwonka
DS, DSE Systems

D. E. Blake
Process Analysis

C. R. Cook, D. J. Moracz
ODSS Systems

Prepared by:

C. F. Barth
Program Manager

W. D. Brentnall
FRS Systems

Approved by:

I. J. Toth
Department Manager

T. S. Stelson
Cost Models

SUMMARY

A rigorous analysis was conducted to estimate relative manufacturing costs for high technology gas turbine blades prepared by three candidate materials/process systems. The three systems examined were: directionally solidified eutectics (DSE), an oxide dispersion strengthened superalloy (ODSS), and a fiber reinforced superalloy (FRS). The manufacturing cost estimates were made employing a turbine blade in current production manufactured of directionally solidified (DS) alloy MAR-M 200 + hafnium to establish baseline data for comparative purposes. The primary program objective was to identify major cost drivers for each materials/process system to provide more efficient use of further process development efforts.

A detailed analytical cost model was developed to quantitatively perform the analysis. The impact of individual process yield factors on cost centers was assessed as well as the influence of process parameters, raw material costs, labor content, and consumable items. The influence of blade design on cost bias towards a particular material/process system is also discussed. For example, increasingly longer airfoil lengths would mitigate against the DSE system while significant airfoil overhang over the root attachment makes both the ODSS and FRS systems less attractive economically.

At least three major cost drivers were identified in terms of total manufacturing costs for each of the advanced materials/process systems examined. The specific process cost drivers and their respective percentages of the total manufacturing cost are tabulated as follows:

Process System	Cost Driver	Percent of Total	
DSE (γ-γ'+α)	Casting	45	84
	Pattern Preparation	26	
	Coating	13	
ODSS (INCO Alloy D)	Root Assembly	37	79
	Coating	23	
	Raw Material & Forge	19	
FRS (FeCrAlY-W)	Root Exert and Assemble	29	87
	Ply Stamp and Assemble	23	
	Tungsten Fibers and Collimation	22	
	Machine and Finish	13	
DS(MAR-M-200+Hf)	Coating	27	62
	Pattern Preparation	25	
	Machining	10	

The major cost drivers amount to 84, 79, and 87 percent of DSE, ODSS, and FRS materials/process systems manufacturing costs, respectively, hence providing some well defined areas for cost reduction activity. It is also significant to note that the major DS cost drivers are not large individually and total only 62% of manufacturing costs.

The remaining 38% is composed of operations each contributing less than ten percent to total costs. The fact that relatively large costs centers exist in the high technology materials/process systems compared to the mature DS system implies that their respective manufacturing costs can be reduced through well-directed efforts in the critical areas identified. A number of these implications are discussed as potential process cost reduction concepts.

The detailed cost model derivation and yield/factor definitions are discussed in an Appendix to this report.

TABLE OF CONTENTS

1.0 INTRODUCTION

NASA is currently sponsoring research on three advanced materials/processing systems that could eventually be utilized in aircraft engine turbine blades with higher temperature capabilities. These three advanced systems are:

> Directionally-solidified eutectics (DSE), which are two-phase cast composites with a grown-in-place high-strength phase reinforcing a more ductile superalloy matrix phase;
>
> Oxide-dispersion-strengthened superalloys (ODSS), which are powder-metallurgy composites that combine the good high-temperature strengthening of fine oxide dispersoids with a γ'-strengthened superalloy matrix for good intermediate-temperature properties; and
>
> Fiber-reinforced superalloys (FRS), which are synthesized composites that utilize high-strength refractory-metal fibers to reinforce an oxidation-resistant superalloy matrix.

All of these systems employ the common feature of providing a directional reinforcement phase to enhance the high-temperature strength capabilities of the composite material. So on a strength basis, all of the systems offer potential improvements in maximum use-temperature for turbine blades. The degrees of improvement potentially available are illustrated in Figure 1 which shows typical strength plots (density compensated) of current material candidates for each of these systems. For comparison, a plot is also shown for a directionally solidified (DS) superalloy, used in turbine blades of current commercial aircraft engines.

Each of the advanced systems are in the early stages of development. So much more work is needed on all of them to mature the materials and processes before the potential turbine blade improvements can actually be realized. In particular, considerable effort is needed in developing cost-effective manufacturing processes. Each of these three systems involve advanced fabrication processes for which very little turbine blade manufacturing experience exists. So the potential manufacturing costs of turbine blades produced by any of the processes is currently open to conjecture. Therefore, NASA contracted TRW to utilize its corporate experience with each of these advanced systems in quantitatively analyzing the systems and defining probable manufacturing processes for each. The prime intent of this study was to identify the operations in each manufacturing process that were likely to be the major cost-drivers. This would help spotlight processing operations where future research emphasis should be concentrated.

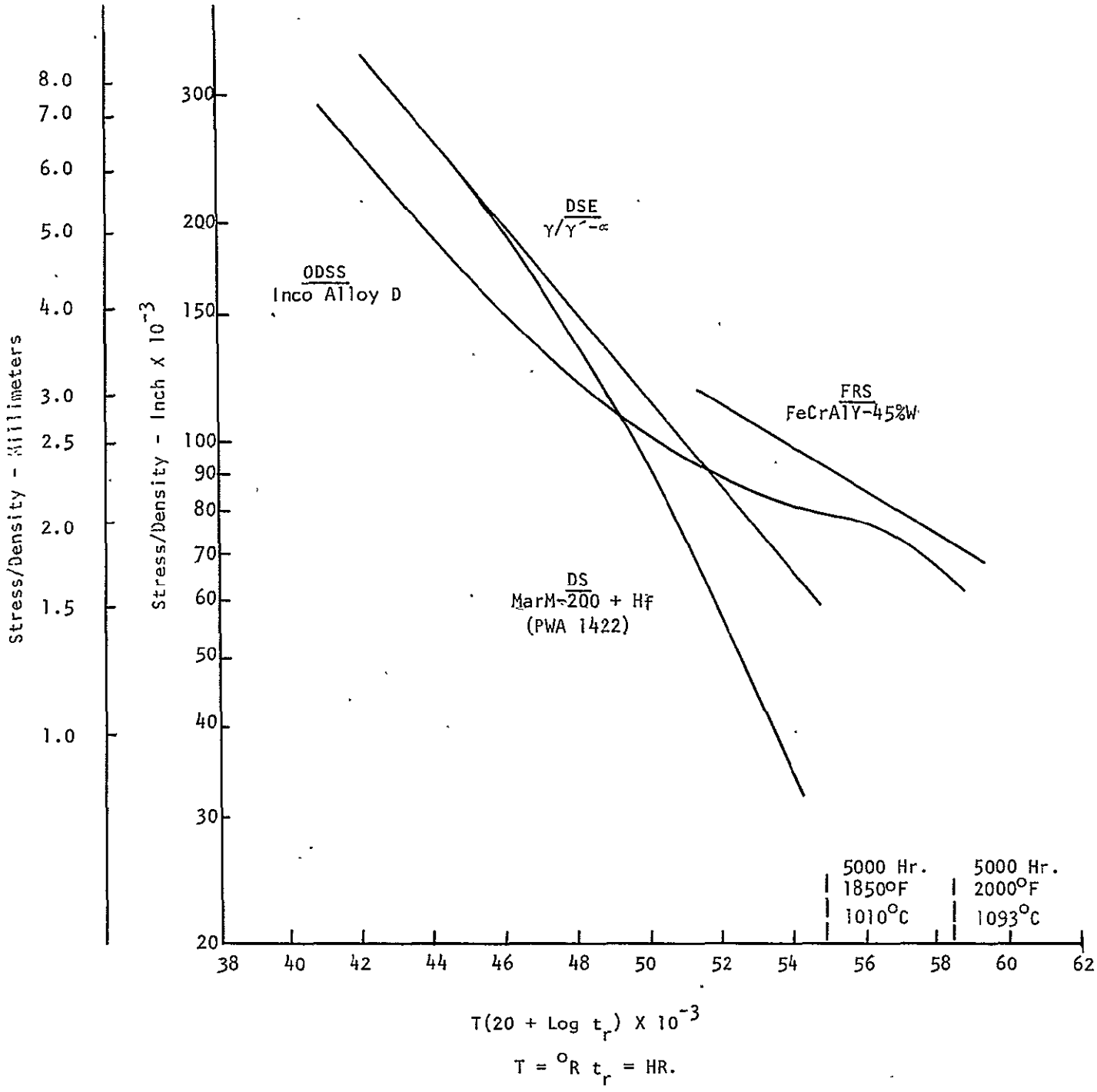

Figure 1. Comparative (Density-Normalized) Larson-Miller Stress-Rupture Curves (Longitudinal Properties) for the Advanced Turbine Blade Materials/Process Systems considered in this study.

The study utilized a cost-modeling technique previously developed by TRW. This technique involved the development of detailed process simulation models for each system and the subsequent calculation of possible manufacturing costs associated with each step in the various processes. A single turbine blade configuration was used for analyzing all of the systems, and some common assumptions were made regarding future development status, production quantities, financial rates, etc. The resulting manufacturing costs were calculated on a relative basis using current commercial practices for directionally-solidified (DS) superalloy turbine blades as the baseline for comparison. This report summarizes the model development, assumptions involved, and relative costs predicted from the analysis.

2.0 BACKGROUND

The three advanced systems are fundamentally similar in the sense that all rely on an aligned secondary phase to impart improved mechanical strengths along the longitudinal blade axis. The manner in which this is accomplished varies significantly, however, for the three materials/process systems under evaluation. A brief review is presented of the major features characterizing the three candidate high technology fabrication methods as well as those of the baseline DS process.

2.1 Directionally Solidified Superalloys

The objective of applying directional solidification to superalloy turbine blade fabrication is to eliminate grain boundaries transverse to the major stress axis. Two important reasons for this approach are that high temperature stress rupture failures occur by a grain boundary sliding mechanism and that crack nucleation by thermal shock effects will preferentially initiate at grain boundaries. Hence, elimination of transverse grain boundaries sharply improves airfoil performance. All alloy systems are not suited for directional solidification processing. This is because in some cases brittle secondary phases precipitate between secondary dendrite arms which are normal to the major stress axis. It is necessary to carefully select superalloy compositions and their resultant solidification habit to develop maximum benefit from directional solidification. The alloy, MAR-M-200 + Hf (PWA 1422), has been particularly amenable to DS processing.

To achieve directional solidification, thermal gradients must be maximized in the desired growth direction and minimized in all other directions. Ideally all heat is extracted from one end of the casting by a chill, which may either be a solid heat sink or embody water cooling. A number of methods have evolved to provide axial heat flow patterns. These include the gradient coil method, exothermic mold packing, and movement of a heat source and chill relative to the solidifying casting. The latter method is used in this study for the cost analysis of DS superalloy turbine blades. Refinements in the process have included radiation shields between the hot and cold zones, careful control of metal superheat, and serrated chills to improve heat extraction. Growth rates up to twelve inches per hour have been realized on multipiece molds by these techniques.

Major problem areas in commercial production of turbine blades by the DS process are: control of the gradient to produce properly aligned structures; and control of core position for internally cooled airfoils. Mold and core materials must also withstand attack by the liquid metal for longer times to preserve the surface integrity of the net shape airfoil geometry. The latter condition is important when it is considered that solidification times for DS parts are extended over conventional equiaxed casting procedures.

2.2 Directionally Solidified Eutectics

One of the major problems of superalloys is the property degradation at high operating temperatures. This property loss is due to the thermodynamic instability of the strengthening phases at these elevated temperatures. Thermodynamic instability is a major limitation to the increasing use-temperatures of superalloys and artificial composites.

A new class of turbine blade materials emerged when eutectic alloys were produced by DS processing. The strengthening, or reinforcing, phase in a eutectic alloy is thermodynamically stable up to the eutectic point temperature. Directionally solidified eutectic (DSE) alloys for turbine blade applications are essentially composites grown from the melt. These alloys are of a nickel-base superalloy matrix reinforced by an aligned high-strength phase. The desired aligned structure is achieved by closely controlling the ratio of the thermal gradient at the solidification front, G, to the rate of advance of the front, R. With increasing G/R, the alloy structure shifts from equiaxed to columnar to cellular dendritic, and finally, above a critical value of G/R, to a fully-aligned eutectic structure (coupled growth).

The G/R ratio may readily be increased by either increasing the thermal gradient, G, or decreasing the growth rate, R. The economics of processing dictate that G be increased as much as practically and physically possible to permit a corresponding increase in R. Higher growth rates also reduce the spacing between the reinforcing phases and thereby provide an improvement in strength properties.

The first generation DSE alloys, γ/γ'-δ and NiTaC-13, have only limited use possibilities, either because of low thermal fatigue resistance and creep shear strength, or because of segregation and mold/core compatibility problems, respectively.

Thus, a promising second generation DSE alloy, γ/γ'-α , is now being studied (reference 1). This alloy has Mo fibers (grown in-situ during casting) as the reinforcing phase. The approximate basic ternary alloy composition, in weight percent, is 30 Mo - 7 Al - balance Ni. Other elements are being added to provide improvements in various properties, such as strength and oxidation resistance. This alloy appears to overcome several of the major problem areas of the first generation alloys and was used to represent DSE alloys in this study.

Mold/melt interactions due to a high superheat temperature are not expected to be as great a problem with γ/γ'-α than with the first generation alloys since its melting point is 1305°C, only about 45°C higher than γ/γ'-δ and 80°C lower than NiTaC-13. However, growth rates are expected to be low - about 1 to 1.5 cm/hr.

All DSE systems are expected to need surface-protective coatings to improve their resistance to the engine oxidizing environment. Coating requirements for γ/γ'-α are (as with other blade materials) dependent upon the temperatures to which they will be subjected. Normally, a blade of the selected design would not be subjected to temperatures which would require this alloy to have an internal coating. However, to take full advantage of its strength capabilities, the γ/γ'-α alloy would be subjected to temperatures which would probably necessitate internal coatings. Thus the need for both external and internal coatings was assumed for this study. The development of these internal and external coatings for this alloy will be required.

2.3 Oxide Dispersion Strengthened Superalloys

Another route to improving the maximum use-temperature of high technology turbine blading is through dispersion strengthening. In this case, a superalloy matrix is preferentially strengthened in the longitudinal direction by an aligned inert oxide dispersoid phase. Thermodynamic stability of the dispersoid with respect to the matrix alloy provides improved elevated temperature stability of the matrix strengthening phase. Another advantage of the oxide dispersion strengthened (ODS) materials is their improved resistance to thermal fatigue. This advantage can be up to tenfold over conventional alloy systems for thermal fatigue related crack propagation.

The current class of advanced ODS alloys, e.g., NiCrAl-oxide exhibit a significant strength advantage over conventional superalloys at 1100°C, (2012°F) and above. However, the lack of intermediate temperature (750°C, 1382°F) strength makes these alloys unacceptable for turbine blade applications. The ODS systems are currently being further developed using mechanical alloying of high-strength superalloy powder and yttrium oxide dispersoids. These are referred to as oxide dispersion strengthened superalloy (ODSS) materials. (2). The superalloy powder matrix is designed to provide the intermediate temperature (760°C, 1400°F) strength by a γ' dispersion and solid solution strengthening. A careful balance of alloy composition is also required to assure some oxidation and sulfidation resistance. Examples of some current nominal alloy compositions are presented in Table II.

TABLE II

Examples of ODS and ODSS Alloy Compositions

Material Designation	Composition, W/O
Huntington MA 757	Ni-16Cr-4Al-0.5Ti-0.6Y_2O_3
Huntington MA 956	Fe-20Cr-4.5Al-0.5Ti-0.6Y_2O_3
INCO Experimental Alloy D	Ni-15Cr-4.5Al-2.5Ti-2Mo-4W-2Ta-0.5C-1.6Y_2O_3

The Huntington materials are semi-commercial alloys which are now available. The INCO alloy is an experimental alloy currently under development and evaluation. The INCO alloy and alloys of this type are being developed for turbine blade applications. It is these latter types of experimental alloys that are of interest to this cost analysis program. The composition of the INCO Alloy D was used in this study.

The basic sequence of ODS preparation involves mechanical alloying - attriting the matrix powder with the dispersoid phase. This procedure incorporates the dispersoid phase within the powder particles rather than merely coating the matrix alloy particles. Consolidation can be accomplished by extrusion in mild steel containers at temperatures in the range of 1900 - 2100°F at high extrusion ratios (for example 16:1). Tooling and preform shapes for secondary processing of ODSS alloys into airfoil configurations must be designed to limit metal flow to the longitudinal direction to maintain the desired texture. Development of such processing technology is essential to reduce airfoil costs associated with procedures involving machining from bulk bar stock. Loss of material in the form of chips wastes a great deal of high cost raw material in addition to requiring extensive NC milling operations. TRW is currently developing near-net forging technology for ODS alloys (Ref. 1,2). The ODS alloys have been found to be extremely strain rate sensitive and in order to process some of these alloys successfully, small reductions per forging pass (less than 25%) are required. The iron-base ODS alloys have been found to be more amenable to net or near-net processing procedures for airfoil fabrication; however, these alloys do not have the thermal fatigue capabilities of their nickel counterparts. It is anticipated that the ODSS materials will be at least as difficult to work into airfoil shapes since superalloys in general are not readily workable.

In summary, therefore, the advanced ODSS materials offer the strength capabilities required of turbine alloys that were not found in today's ODS materials; however, ODSS materials do not have the oxidation resistance of the ODS materials and will probably have to be coated. (This study assumed that coatings would be required on both the external and internal surfaces of ODSS blades.) In addition, the fabrication of these materials into airfoil shapes will require the development of a processing technology similar to the ODS materials.

2.4 Fiber Reinforced Superalloys

Fiber reinforced superalloys (FRS) have been under development for the past six to eight years. These programs have identified several promising alloy/fiber systems and in particular have identified a tungsten-wire-reinforced/FeCrAlY matrix composite system as having potential for use in future gas turbine engines. Primary applications for these composites are anticipated to be turbine blades.

In preliminary development work, fabrication parameters were identified and screening studies were performed using a variety of potential reinforcements. Based on elevated temperature compatibility, preliminary stress rupture data, cost, and material availability, refractory metal wires of either tungsten or molybdenum alloys were identified as having the greatest potential as reinforcements for first generation FRS systems.

The W-1ThO_2/FeCrAlY* composite FRS system was subsequently shown to have potential long-term (>1000 hour stress rupture) life at temperatures up to 1150°C (2100°F). The oxidation/sulfidation resistance of the FeCrAlY matrix seems such that protective surface coatings should be unnecessary on W/FeCrAlY composites. Thus, this study assumed that no surface coatings would be required on FRS blades. Additionally, the resistance to thermal cycling and low cycle fatigue (LCF) damage at temperatures and stress levels representative of turbine blade requirements appears to be adequate.

Solid-state diffusion bonding fabrication methods are being developed to fabricate these composites from pre-consolidated monotapes which utilize wrought sheet or pre-alloyed powder matrix materials (FeCrAlY). The reinforcement consists of continuous tungsten fibers which are accurately collimated by a drum winding process. Consolidation of the matrix alloy about the collimated fibers produces single or multi-layer composite panels, now described by the term, monotapes. The powder cloth process in which alloy powders are converted (by use of suitable plasticizers) to highly flexible sheets having excellent handleability is a critical element of the current processing technology. Specific advantages of this approach involving powder cloths and collimated fibers consolidated by solid state diffusion bonding include the following:

1. Fiber/matrix reactions are minimized,

2. Fiber properties are not significantly degraded during processing,

3. Precise control can be exercised over fiber distributions and volume fractions,

4. Fiber orientations can be readily controlled to provide strengthening in several desired directions, and

5. The process is amenable to fabrication of complex, three-dimensionally-contoured shapes.

*Nominal Alloy Composition Fe-20 to 25% Cr-5%Al-0.5 to 1%Y

The major obstacles to engine test qualifications of FRS alloys are the need to more fully develop prototype hardware fabrication sequences to demonstrate the cost effectiveness of the blade fabrication procedures and to optimize the thermal fatigue properties of FRS blades. Also, design means to cope with the higher absolute density of these composites must be developed. Therefore, considerable effort remains to design, develop, and test prototype configurations before the potential offered by the FRS composite system can be realized.

2.5 Quantitative Process Analysis

A comprehensive research program has been in progress at TRW to develop quantitative methodologies for systematic analysis of manufacturing operations involving metal removal. The program initially addressed grinding procedures for superalloy materials used in turbine blade manufacturing operations. The objective of this early work was to establish systems of parametric equations to relate machine operation and part quality to manufacturing cost.

It was soon apparent that a quantitative means was required to compare the cost effectiveness of recommended process changes to past or current practices. The development of the cost modeling concept was a natural outgrowth of this need. It was necessary to realistically define the cost/benefit effects of potential improvements in grinding and machining technology. Hence the cost model provided the yardstick to rigorously perform such comparisons. It was also apparent that cost modeling procedures would have application in support of a variety of manufacturing-related operations involving procedures other than those strictly related to metal removal. Thus, these modeling techniques were subsequently applied to the entire spectrum of processing steps involved in turbine blade manufacture.

3.0 TECHNICAL APPROACH

Determination of fabrication costs for high technology turbine blades using the three candidate materials/process systems was made by employing the TRW-developed process analysis and cost modeling technology. The overall technical approach to the problem is reviewed in detail to define the constraints, assumptions, and boundary conditions used in the model development.

3.1 Component Selection

Selection of a common part design is absolutely essential in developing an equitable manufacturing cost comparison for the three materials/process systems for high technology turbine blading. The selection process also involves a recognition of potential bias effects for or against any of the three candidate systems. For example, a blade design having a large trailing edge overhang with respect to the root attachment can mitigate against the FRS system while relatively long airfoils sharply increase DSE fabrication costs. A third factor involves providing a benchmark of well-defined properties against which to compare the relative cost/performance benefits afforded by the candidate advanced technology blade fabrication systems.

After careful consideration of the above factors, a JT9D-7F first stage turbine blade configuration was selected as the component to be utilized in the manufacturing cost analysis. The part was selected for the following three reasons:

1. This blade is currently in production for a commercial aircraft engine using the directionally solidified (DS) process;

2. The part is characteristic of current state-of-the-art technology levels;

3. The blade design, with its moderate trailing edge overhang and approximate four-inch length affords no singular advantage to either of the three candidate systems;

A photograph of the turbine blade selected is presented in Figure 2, as it appears prior to the root finishing operations. Some of the important features of this design include trailing edge cooling passages, some trailing edge overhang with respect to the root attachment, and an overall length of approximately 10cm (4 in). The existence of internal cooling passages and use of numerous air exit holes provides a reasonable challenge for all three candidate systems to produce a hollow component. The second feature involving a reasonable amount of trailing edge overhang facilitates producibility by either the ODSS or FRS systems while the moderate overall length does not seriously compromise the DSE process economics.

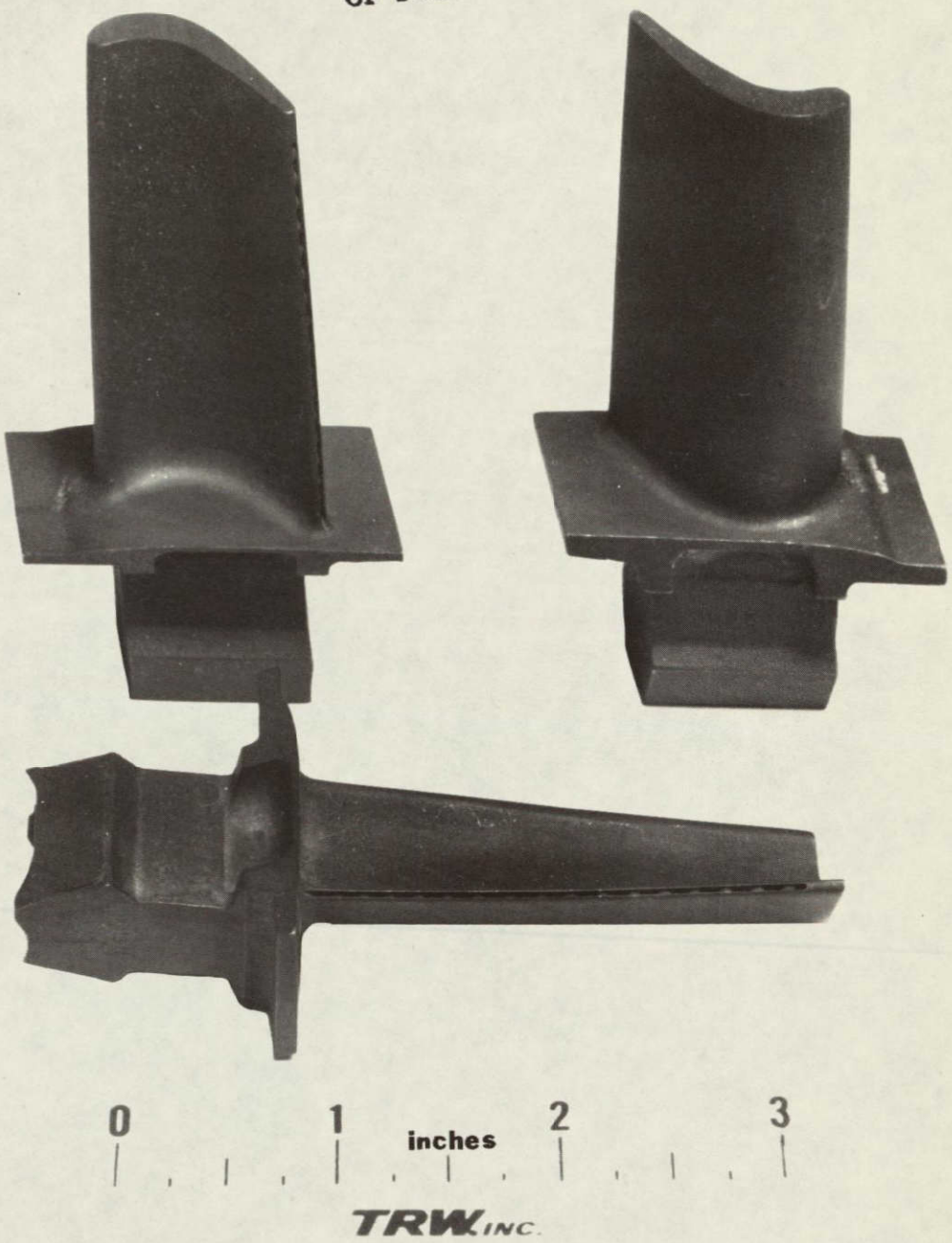

Figure 2. Overall appearance of the Turbine Blade Configuration used in this study.

3.2 Basic Process Assumptions

Realistic manufacturing cost comparisons between the established DS process and the three candidate materials/process systems now under development require that a number of fundamental assumptions be defined. These assumptions relate to the conditions surrounding extrapolation of this technology from the laboratory stage into a simulation of full production. For example, it is necessary to assume that the various processing steps involved in fabrication of a blade by a given method have fully matured. At the present time, mold materials for the DSE process do not have optimum refractory properties to sustain the liquid metal temperatures required to develop the desired thermal gradient needed with some DSE alloys and must be assumed to have been developed. The maximum metal temperature can be increased in service as a result of improved mechanical properties; hence, oxidation resistance becomes a more critical factor. Coating systems for blades manufactured by the ODSS and DSE systems require further development in order for these materials to be used at their maximum use-temperature. Thermally induced stresses between the fibers and matrix of the FRS structures at elevated temperature must be evaluated as well as nondestructive inspection procedures for internal defects in both FRS and DSE processed blades.

On the tacit assumption that problems of the nature discussed in the preceding paragraph have been resolved, a series of process model boundary conditions were established. These conditions are summarized as follows:

1. The manufacturing lot size considered is 2000 pieces;

2. A total of 500 engine sets have previously been commercially produced;

3. Capital equipment and specialized tooling or fixtures have been amortized during the 500 engine set production;

4. Costs associated with maintaining capital equipment, die resinking due to wear, and mold making facilities, etc., during the production run have been included in the overhead burden; and

5. Process yields for operations involving manufacture of these high technology parts are at least comparable to those presently observed for similar state-of-the-art techniques.

The preceding boundary conditions represent a reasonable basis for preparing accurate cost models to simulate costs associated with full-scale component manufacture.

3.3 Process Definition

The development of detailed processing steps involved in the fabrication of each candidate materials/process system are treated in this section. Both the process flow chart development and the rationale behind each particular step are reviewed sequentially. The basic concept involved resolution of the seemingly complex manufacturing sequences into successively finer detail until each discrete step could be reliably modeled mathematically. Only one fundamental limitation was observed: no process step would be defined in greater detail than the reliability of the assumptions involved. For example, if further resolution of an element of an individual process step only changed the cost estimate for this step by less than 1%, it was not performed.

The preliminary analysis established that all four materials/process systems share a common series of four overall manufacturing steps. These steps are: (1) fabrication, in which the basic airfoil geometry is generated; (2) machining where the root attachment details are produced; (3) coating; and (4) final acceptance inspection prior to shipment to the user. A combined flow chart describing an overview of these operations is presented in Figure 3 for the DS, DSE, ODSS, and FRS systems. Each of the blocks presented in this flow chart of themselves represent a series of manufacturing sequences necessary to fabricate the turbine blade. A second commonality, which is indicated in Figure 3, is that all four materials/process systems differ primarily only in the initial fabrication step. The fabricated airfoil shape at the end of this step is virtually identical for all systems under evaluation. The major differences in process costs for all succeeding operations arise from different responses to grinding stresses and the type or need for a coating system. Final acceptance inspections are identical in all cases. Hence, while all blocks defined in Figure 3 will be discussed in detail, the major emphasis will logically be on the initial fabrication procedures.

3.3.1 Directionally Solidified Superalloys - Fabrication

The fabrication sequence currently used for production of the selected turbine blade by the established DS process is presented in Figure 4. The discrete labor operations, raw materials, and consumable items are identified for each block in this sub-section. This overall fabrication sequence is presented without comment or assumptions required because it is a description of an existing production operation.

The wax patterns are first prepared by injection molding processes and contain precision-shaped ceramic cores to provide the internal cooling passage configurations. The only materials actually consumed in this step are the cores which are eventually disintegrated after the blade has been cast. Most of the pattern wax is recovered and recycled. The pattern-making operation includes the actual blade shape as well as other mold parts such as gates, runners, risers, sprues, and the pouring cup.

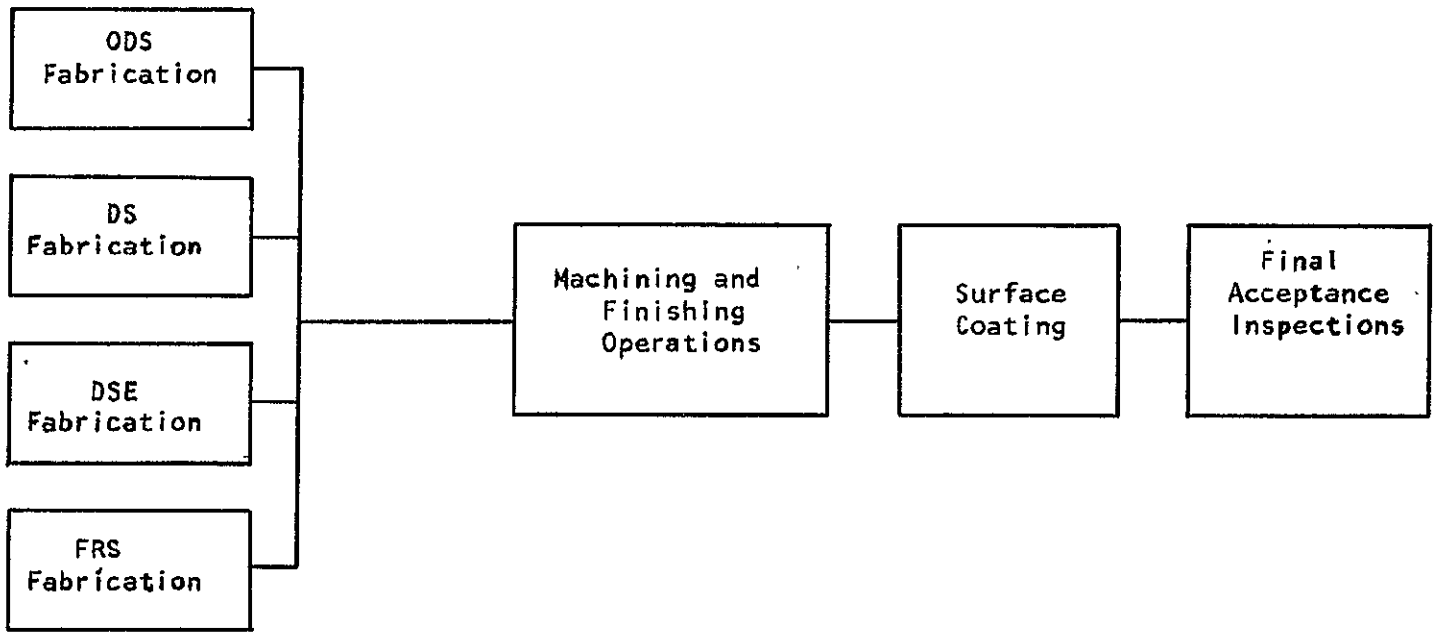

Figure 3. Overall Process Flow Chart

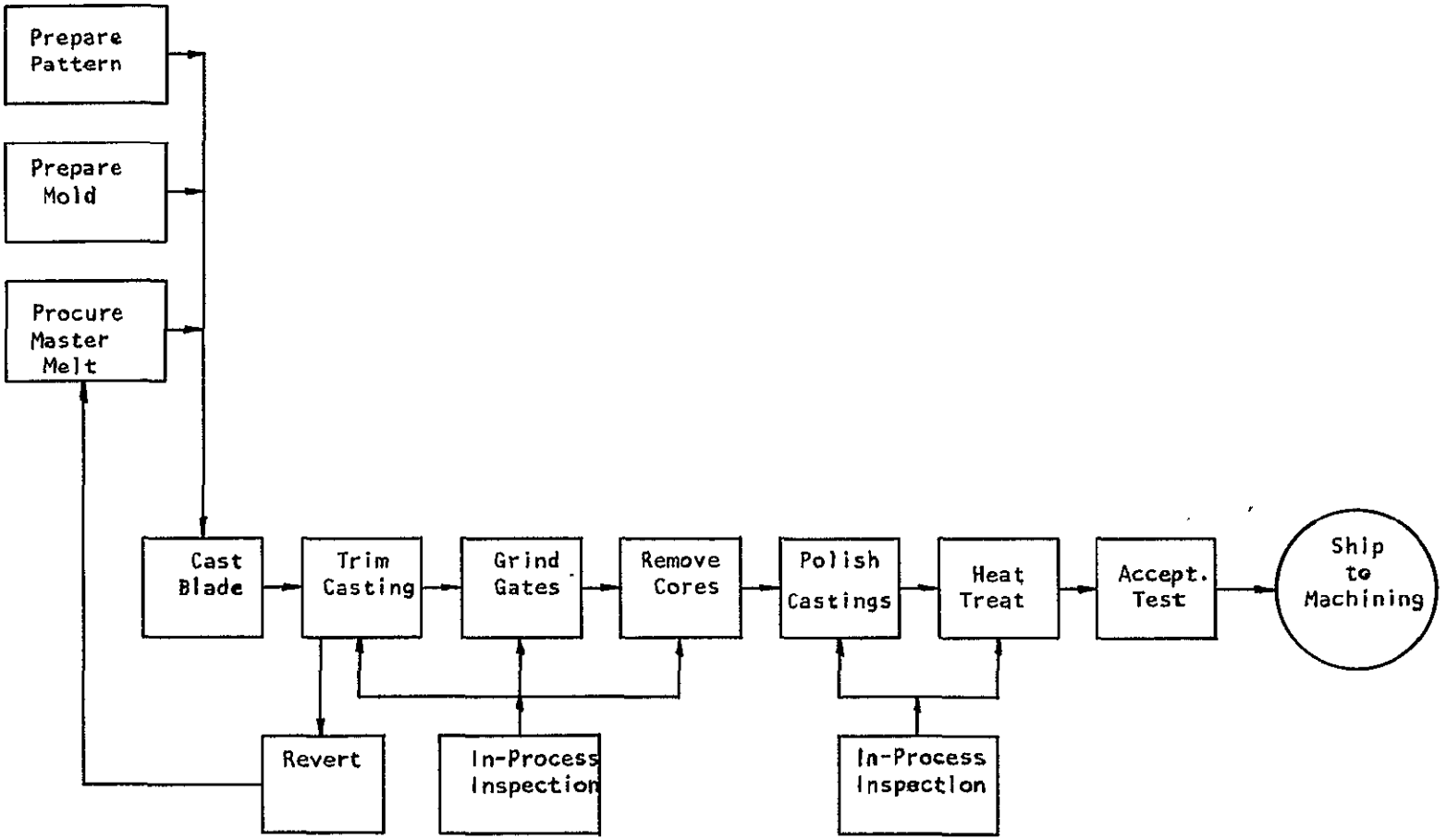

Figure 4. Fabrication Sequence for DS and DSE Turbine Blades

The actual mold is prepared by investing the completed wax pattern in a succession of ceramic dip coatings. After the ceramic structure has been fully built-up, the mold is dried, dewaxed, and fired. The firing process not only develops the desired ceramic strength properties, but it assures complete removal of any residual wax remaining from the pattern.

The alloy to be poured is compounded from carefully-controlled-analysis master melts with accompanying revert alloy recovered as gates and risers from previous heats. Particular attention at this point must be given to elimination of potential contaminants which will later be evidenced as inclusions or defects in the resulting casting.

The actual DS casting operation (by the withdrawal process) is conducted under vacuum to prevent oxidation of active alloy additives. Normally, a two-chamber furnace is utilized with a preheated mold introduced below the melting crucible. These blades are currently cast in clusters of 19 at a time(with a production rate of 19 blades per operator hour). After pouring, the mold is withdrawn under closely controlled conditions through a temperature gradient in contact with a chill at the mold base. The major consumable item in the casting operation is energy.

The solidified casting is shaken out of the mold and the blades are removed from the cluster by a trimming operation. A portion of the cast material is recovered as revert stock and costs associated with the master melt material reflect utilization of the recovered material. Design of the cluster is important to maximize the number of parts produced in a single pour while providing ready means of part separation from the sprue. The principal consumable is cutoff wheels used to section the cluster.

The cast blades are then ground to remove gating prior to processing by autoclaving to remove the ceramic cores. Following core removal, the castings are inspected for external casting defects and complete core removal, the alloy analysis is checked, and the heat code identity is provided. The castings are then subjected to surface conditioning prior to heat treatment. After thermal treatment the blade castings are subjected to fluorescent penetrant inspection (FPI) and further visual inspection for surface defects, particularly at the cooling passage details. Also, the dimensions are inspected against part requirements. The consumable items are relatively minor in these operations with the major emphasis on labor content.

An overall inspection is then performed prior to shipment of the parts for the succeeding operations. The yields and influence of various process elements will be discussed in Section 4.0 as part of the economic analysis.

3.3.2 Directionally Solidified Eutectics - Fabrication

Directionally solidified eutectic blades follow much the same fabrication steps as DS blades. The major difference between DS and the advanced technology DSE fabrication sequence lies principally in the control of the solidification process. The much slower withdrawal rates and stringent temperature gradient requirements for DSE blades require more sophisticated equipment and process controls. In addition the mold and core materials for DSE blades must be of a more refractory nature to resist mold-metal interactions during protracted contact with the molten alloy.

Solidification rates of 6 mm per hour (1/4 inch per hour) were assumed to produce the desired lamellar structure of an off-eutectic composition for the γ-γ'+ α alloy while maximizing the mechanical properties. A further justification for selecting this rare alloy involves difficulties in producing complex blade shapes at rates above 6 mm per hour. Simple shapes can be withdrawn at greater rates, but the section size transitions required at the platform/airfoil interface preclude higher rates.

The DSE blades were assumed to be cast in clusters of 4 units, as compared to 19 in the case of the DS process. However, due to the relatively slow withdrawal rate, an operator can monitor three production units versus monitoring of a single unit for DS blades. This would amount to a production rate of 0.6 blades per operator hour (3 furnaces times 4 blades per cluster divided by 20 hours withdrawal time). The production rate for DS parts is approximately 19 blades per operator hour. Hence the labor costs for DSE casting will be a major factor in the cost analysis. Increases in the withdrawal rate are not as effective in reducing costs as would be an increase in the number of blades cast per cluster. An operator would only be able to tend two DSE furnaces at withdrawal rates of 12 mm per hour (1/2 inch per hour), instead of three at the slower rate. However, doubling the number of blades per cluster would also double labor productivity to 1.2 blades per hour.

The flow chart defined for the DS fabrication process (Figure 4) will be also appropriate for the DSE fabrication process sequence as well. The principal differences will be in the raw materials and the casting parameter data. As will be defined later, yield factors for the various DSE processing elements were assumed to be at least as good as those observed for similar DS elements in current production.

3.3.3 Oxide Dispersion Strengthened Superalloys - Fabrication

The fabrication sequence for the selected turbine blade of an ODSS material primarily involves forging and/or machining procedures. The detailed flow chart developed for this material/process system is presented in Figure 5. The selected alloy, Inco Experimental Alloy D, (Table II) was assumed to be directionally forged into net airfoil configurations. Calculations involving tradeoffs between machining an airfoil directly from bar stock versus the net forging approach revealed the latter is the most cost-effective solution. Hence, the selected processing sequence involves purchase of previously consolidated extruded ODSS preform bar stock which is then precision forged into the net airfoil shape in two subsequent forging iterations. Each iteration is limited to less than 25% reduction to avert cracking. The airfoil forgings are processed to full blade length, extending from the root base to the airfoil tip.

The root block was assumed to be attached in a later operation as a separate piece, as illustrated in Figure 6. This fabrication concept provides several important advantages. The first benefit is that precise control of directional properties can be uniformly maintained along the entire ODSS airfoil length. Secondly, extensive contour machining in the airfoil/platform area is not required. Finally, the use of a root exert of an equiaxed superalloy (e.g. - IN738) casting avoids subjecting the ODSS material to shear stresses in the longitudinal direction at the root serrations. A key factor in the assembly process is the provision of a 10° taper in the lower portion of the airfoil and a matching internal taper in the root exert. The angle provides a self locking feature and relieves the requirement that the brazed joint must support operational stresses in pure shear.

Several operations are performed prior to the assembly operation described above. The blade must be ground to length, the leading and trailing edges accurately blended, and the root area tapered to accept the cast root exert. The internal cooling passages are also produced by a combined electrochemical machining (ECM) and electrostream drilling operation. The axial cavity is first generated by ECM from the root end, and then the trailing edge holes are drilled electrochemically to communicate with the internal cavity. After inspection, the internal surfaces are coated with a pack diffusion coating to provide oxidation resistance during engine operation.

At this point the hollow airfoil, the root exert, and a cast cooling tube assembly are vacuum brazed into an integral unit. Another series of inspections are performed to assure proper airflow through the cooling passages and to verify proper registration of the airfoil and root block. The ODSS blade now resembles almost exactly the appearance of the cast DS or DSE components and can be shipped to the next sequence in the machining and finishing process, in which the root details are generated.

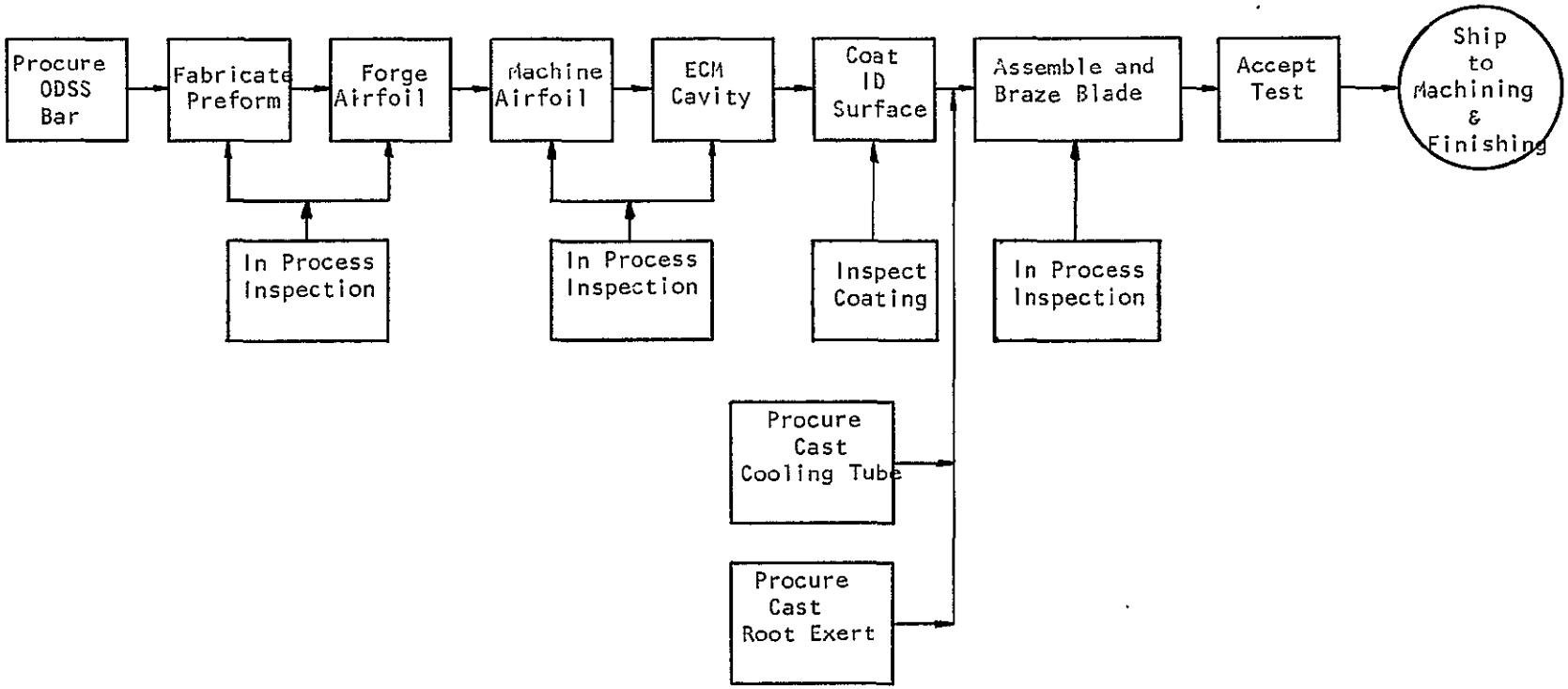

Figure 5. Fabrication Sequence for ODSS Turbine Blades

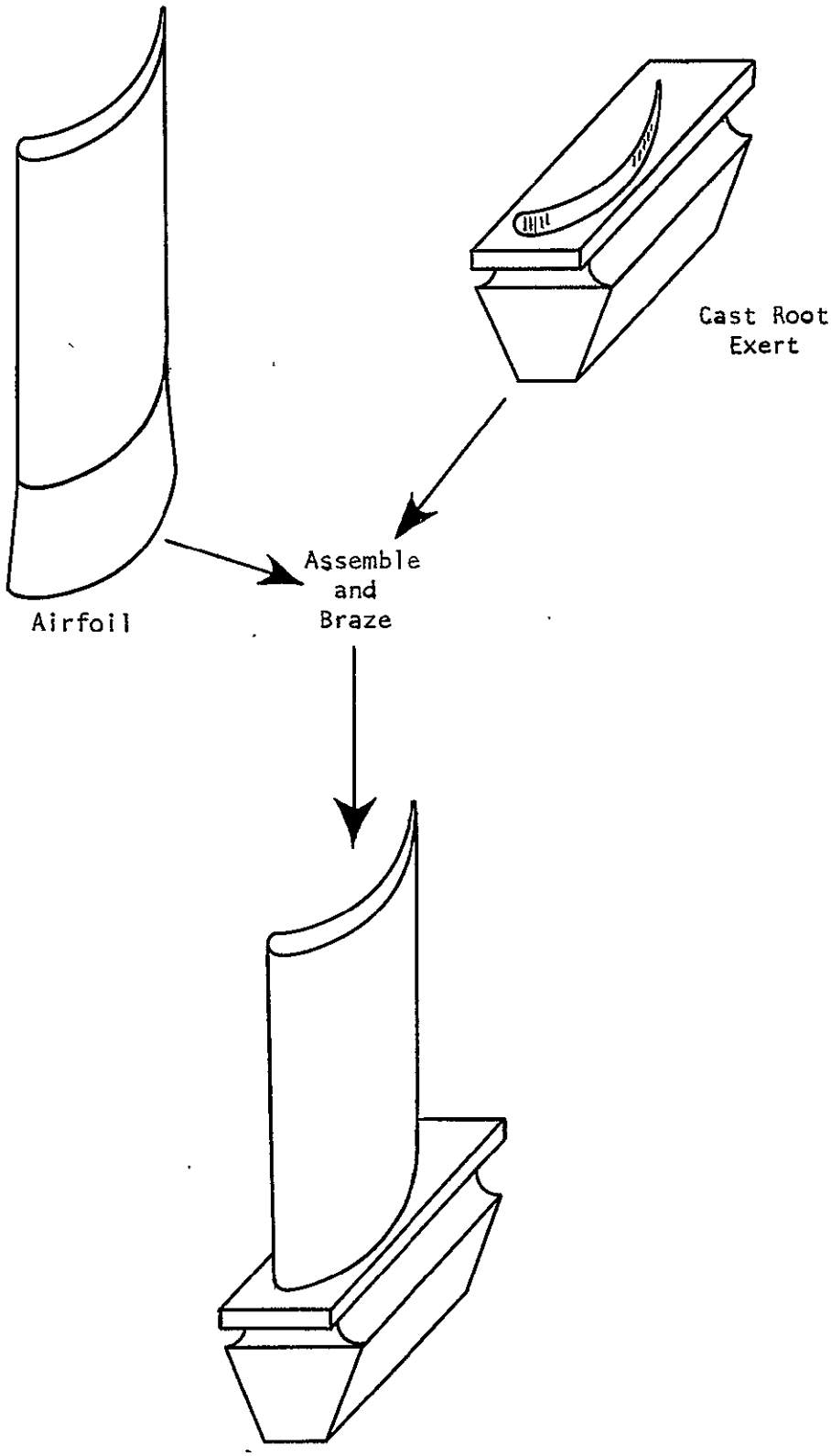

Figure 6. Illustration of concept of root exert attachment on an ODSS or FRS airfoil.

3.3.4 Fiber Reinforced Superalloys - Fabrication

Application of the FRS system to fabrication of the selected turbine blade was assumed to involve consolidation of powdered alloy and collimated fibers into sheet form containing one layer of fibers and then hot pressing a layup of plies into an airfoil shape. This process is analogous to those currently used to produce boron/aluminum fan blades for turbine engines. The same concept used in the ODSS fabrication of attaching a cast root exert on the airfoil was also used as a key part of the FRS fabrication sequence (Fig. 6).

The detailed process flow chart for the FRS fabrication sequence is illustrated in Figure 7. The matrix alloy powder (Fe-20 to 25% Cr-5% Al-0.5 to 1% Y) is first blended with teflon and rolled into an extremely flexible powder cloth. The as-rolled cloth is inspected for uniform density and thickness and any material not meeting specification is merely recycled through the blending and rolling operation. Concurrent with the powder preparation, tungsten wires are collimated in a drum winding operation using a polystyrene resin to maintain fiber alignment and provide handleability. The wire mats are removed from the drum and inspected to assure proper collimation.

A sandwich of a wire mat surrounded by two layers of powder cloth is hot pressed to produce a fully consolidated sheet, or monotape. Although an inspection is performed to assure uniform monotape thickness and wire collimation, control of cloth thickness and density prior to consolidation is the primary quality control factor.

A computer program is used to define the number, shape, and orientation of individual monotape plies for generating a particular blade configuration. Hence, the plies are stamped and assembled according to the specific blade design requirements. An iron core is inserted during the ply-layup process to provide for the internal cooling passages. The plies are assembled in a jig with spot weld tacks to maintain precise alignment during the subsequent hot pressing operation. Control of time, temperature, and load are critical to assure full consolidation of the various plies while minimizing any tendency towards degradation of the tungsten fiber properties. For example, exposures to temperatures significantly above 1200°C (2200°F) can lead to loss of tungsten wire properties. This constraint is generally regarded as precluding any casting-type operation to incorporate tungsten wire reinforcement concepts in a DS or DSE process matrix alloy.

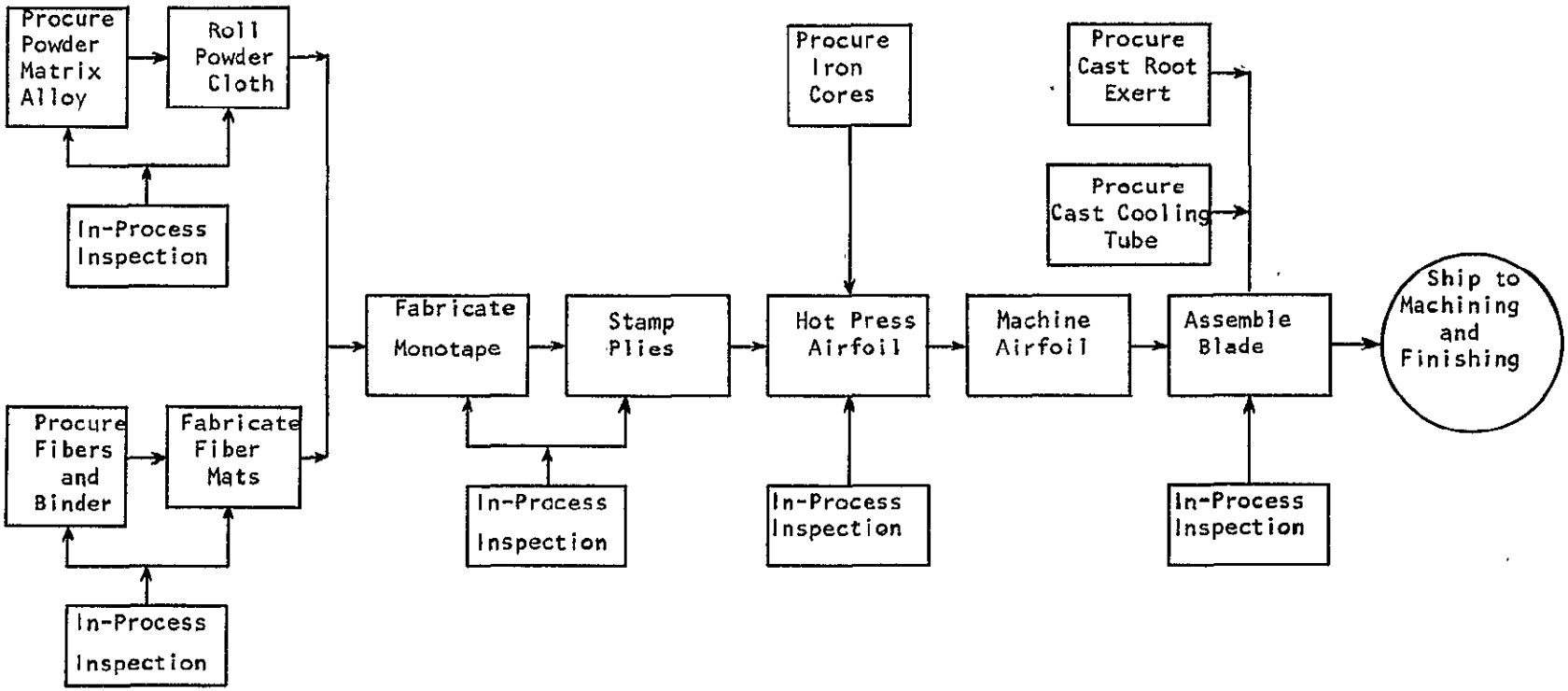

Figure 7. Fabrication Sequence for FRS Turbine Blades

After the hot pressing operation, the iron core is removed by chemical leaching in which tubes are used to pump the acid directly on the receding iron core surface. The hollow airfoil is then subjected to the same series of machining, assembly, and brazing operations as the fabrication sequence developed for the ODSS material/process system. The only difference is that the internal coating of the hollow FRS airfoil is unnecessary owing to the adequate oxidation resistance of the FeCrAlY matrix alloy. Again, the FRS component at the completion of the fabrication sequence closely resembles blades fabricated by the DS process in overall external appearance. The as-fabricated blades are then shipped for machining and finishing operations.

3.3.5 Machining and Finishing Operations - All Process Systems

Components entering the Machining and Finishing Operation would be virtually identical in outward appearance regardless of the fabrication sequence utilized. The objective of this process sequence is to impart the required precision root attachment geometries to the components. In all cases precision form grinding will be utilized to achieve this objective. The major difference between the four materials/process systems will be in the area of grinding parameter variations, wheel life, and crack susceptibility. The latter constraint impacts maximum permissible metal removal rates to preserve surface integrity within acceptable limits.

The detailed flow chart developed for the Post-Fabrication sequence is illustrated in Figure 8. A comprehensive discussion of this sequence is not necessary since all four materials/process systems are subjected to virtually identical procedures. The discussion will focus on differences in grinding responses exhibited by the DS, DSE, and cast superalloy root exerts on the ODSS and FRS materials. Metal removal rates, and hence costs, vary for these materials as summarized in Table III. Although the ODSS and FRS airfoil fabrication sequences do not involve casting, the thermal cycle treatment developed to open any existing grinding or casting defects in cast turbine blades is still required to assure integrity of the root serration ground into the roots exerts.

TABLE III

Grinding Response Comparison

Material/Process System	Root Material	Maximum Depth of Cut per Pass	Relative Grinding Costs
DS	MarM-200+Hf	.076mm (.003 in.)	Intermediate
DSE	$\gamma+\gamma'+\alpha$	.025mm (.001 in.)	Highest
ODSS	IN738	.152mm (.006 in.)	Lowest
FRS	IN738	.152mm (.006 in.)	Lowest

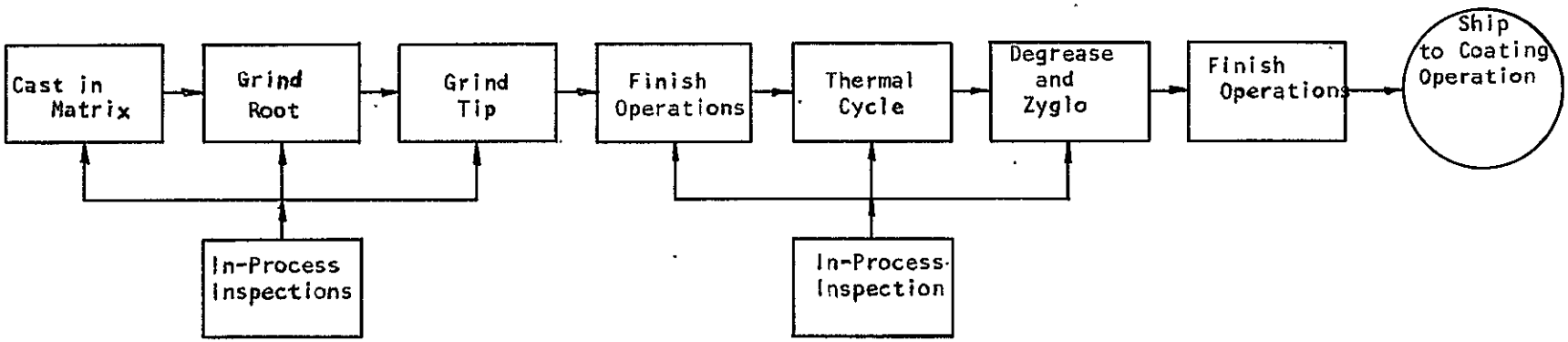

Figure 8. Process Flow Chart for the Machining and Finishing Sequence for all Fabrication Methods.

While the Machining and Finishing sequence represents a major cost center in the overall manufacturing sequence, it is only necessary to quantify this contribution to overall costs and define the influence of grinding parameter variations on this particular cost center. Therefore, the major concern with the Machining and Finishing sequence will be treated in Section 4.1 in which the relative costs are defined. Detailed parameter differences outlined in the cost model equations are presented in the Appendix.

3.3.6 Coating Application - All Systems Except FRS

The coating requirements for each material/process system are summarized in Table IV. The successful use of PVD-CoCrAlY overlay coatings on blades fabricated by either the DSE or ODSS materials/process systems has yet to be demonstrated. It was assumed, however, that this coating or one similar will be developed for application to the respective component fabrication systems. Unless some major application problem is encountered, the costs for overlay coatings for these components were assumed to be comparable to those currently established for the PVD-CoCrAlY system. The assumption that internal coatings were required for blades fabricated by the ODSS or DSE systems was justified by the fact that the current DS part is strength limited. The higher permissible metal temperatures afforded by these high technology materials/process systems will now require a greater degree of protection. Blades manufactured by the FRS materials/process systems exhibit excellent oxidation resistance at metal temperatures up to 1200-1260°C (2200-2300°F) primarily because the matrix is essentially a coating alloy; hence, this material system was assumed to not require a coating.

TABLE VI

Coating Requirements

Material/Process System	External Coating	Internal Coating
DS	PVD-CoCrAlY	None
DSE	" "	Pack-NiCoCrAlY
ODSS	" "	" "
FRS	None	None

The internal coating is a NiCoCrAlY alloy and is applied to the blade surface by a pack diffusion process. The external coating material is a CoCrAlY alloy and is applied by an overlay process involving vapor deposition. Nominal composition of typical alloys of these types are presented in Table V.

TABLE V

Nominal Coating Alloy Compositions

NiCoCrAly		CoCrAly	
Ni	50-56%	Co	68%
Co	20-25%	Cr	20-25%
Cr	12-19%	Al	12-14%
Al	6-10%	Y	0.9%
Y	0.2-0.3%		

The flow chart developed for the coating operations, where they are required, is relatively uncomplicated and is presented in Figure 9. The actual coating procedures are of a proprietary nature, and a great deal of detailed information concerning the specific production details are not generally available. Qualified coating vendors perform the service on a quotation basis. The only information available for this study was that approximately 25% of the parts are rejected from a particular coating run. At the present time, development work is underway to successfully remove defective overlay coatings for subsequent reprocessing. So it was assumed for this analysis that a suitable technique has been devised to reprocess components involving overlay coating operations. This is a critical factor when the value of a high technology blade is considered at this point in the manufacturing cycle. Rejection of a component as scrap will seriously influence the yield factors and, hence, final manufacturing costs.

A minor point in the process analysis sequence involves the internal coating of the ODSS blades. . While the actual coating of the internal cooling passage is performed during the initial fabrication procedures, the costs have been deleted from the fabrication sequence and included as part of the overall coating costs. for the final comparison.

3.3.7 Final Acceptance Inspection - All Systems

Prior to shipment of the completed blades to the engine builder, a series of final inspection operations are performed to assure compliance with specifications. The sequence of inspection operations are virtually identical for all materials/process systems. The inspection operations required are summarized in Table VI.

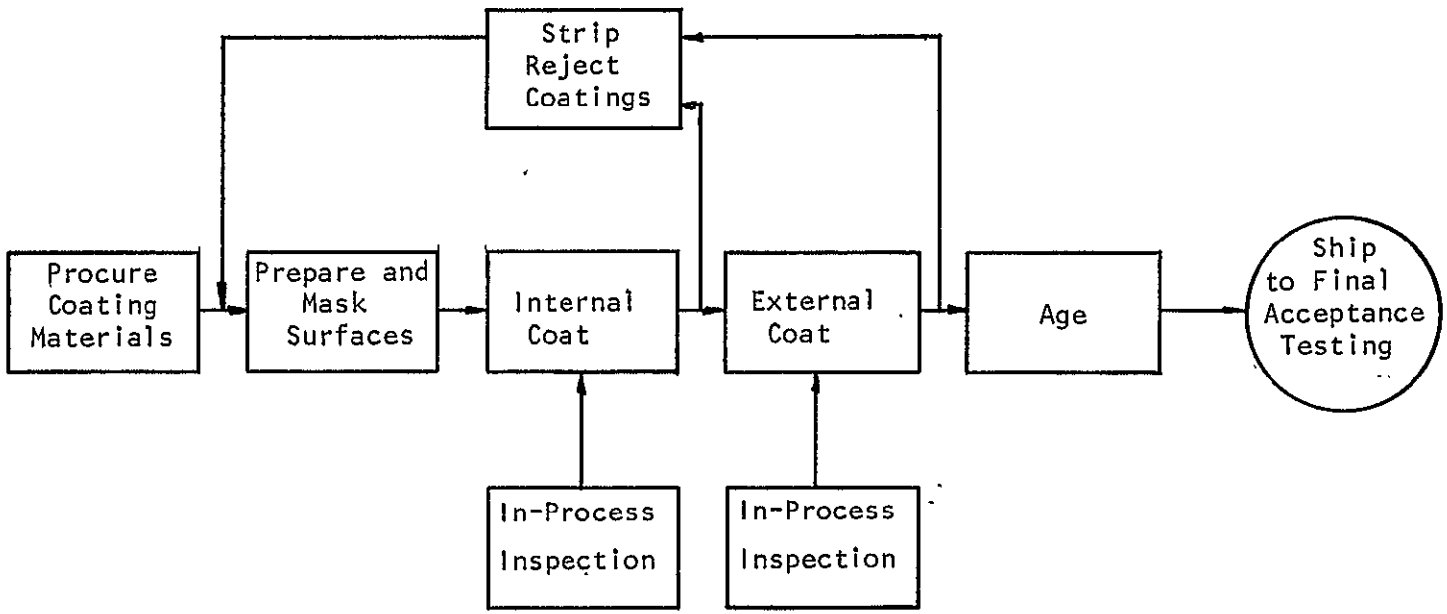

Figure 9. Coating Operation Sequence.

TABLE VI

Final Acceptance Inspections

Operation	Purpose
Dimensional	Compliance with required geometry specs.
Alloy Composition	Proper Chemistry
Cooling Passages	
a. Airflow	Unobstructed airflow pattern and volume
b. Coating	Proper protection
c. Contamination	Residual Core Removal Check
Part Identity	Serialization and Traceability
Visual	Mechanical Handling Damage

Since components fabricated by any of the four materials/process systems must be subjected to the same inspection, the costs will be the same. It is primarily necessary to define this cost as a part of the overall manufacturing costs and is not expected to seriously influence any differences in the relative process cost comparisons.

4.0 ECONOMIC ANALYSIS

The primary program objective was to analyze each of the three candidate materials/process systems such that major cost drivers could be identified. To achieve this objective, detailed manufacturing cost estimates were prepared using mathematical process models for each process step defined in the flow charts developed in Sub-Section 3.3. The actual model development and treatment of the yield factor questions is presented in detail in the Appendix. This fundamental information was necessary to provide the basic background algorithms for eventual cost driver identification. This section will examine the complex cost data developed from the process models. All cost data were normalized with respect to the manufacturing cost for blades fabricated by the DS process. The cost drivers for each candidate system were then extracted and presented in terms of percentages of the total manufacturing cost for that materials/process system.

4.1 Cost Analysis

A summary of the detailed process cost elements are presented in Tables VII through X for the DS, DSE, ODSS, and FRS materials/process systems, respectively. The data presented in these tables are relatively complex and the significance of each column heading will be described prior to a detailed analysis of the results. The specific nature of each column is described as follows:

Column 1 - Manufacturing Steps - The four basic process operational blocks previously identified in Figure 3 are listed with a detailed breakdown of the individual process block elements. These elements reflect the various process steps comprising the manufacturing operation.

Column 2 - Normalized Costs - The normalized cost data are presented in two sub-columns. The first subcolumn represents individual process cost elements required to produce one good blade without scrap for each process operation. The second subcolumn illustrates the arrangement of cost centers and associated inspection operations necessary to apply yield factors to obtain realistic cost estimates for production. The total cost for the DS process at 100% yield was set equal to an index of 100 and all other cost estimates were normalized with respect to this value.

Column 3 - Yield Factors - The factors tabulated in this column represent the expected or actual yields for each operation in the manufacturing sequence. In some cases, an operation has been assigned a separate yield factor while others illustrate the coupling effects of several manufacturing operations followed by an inspection. In the latter instance, the inspection step identifies the fraction of rejectable parts produced by any or all of the associated manufacturing operations.

TABLE VII

Baseline Manufacturing Costs for DS Blades

1. Manufacturing steps	2. Normalized Costs @ 100% Yield: Individual Elements	2. Normalized Costs @ 100% Yield: Coupled Processes	3. Yield Factor	4. Process Cost at the Yield	5. Number of Operations Required	6. Actual Step Costs Per Part	7. Cumulative Value	8. Added Value of Step
Fabrication								
Prepare Pattern	7.71	7.71	.80	9.64	5.93	45.72	9.64	9.64
Prepare Mold	.86	.86	.95	.91	4.75	4.09	11.05	1.41
Master Melt & Revert	2.05	2.05	1.00	2.05	2.71	5.56	13.10	2.05
Cast	3.62	3.62	.60	6.03	4.51	16.33	26.50	13.40
Trim	.48							
Grind Gate	1.28	4.50	.80	5.63	2.71	12.20	38.75	12.25
Remove Core	.10							
Inspect	2.64							
Polish	5.99							
Heat Treat	.13	7.17	.80	8.96	2.16	15.49	57.40	18.65
Inspect	.95							
Acceptance Evaluation	4.30		.80	5.38	1.73	7.44	77.13	19.93
Machining and Finishing								
Cast in Matrix	1.78							
Grind Root	2.46							
Grind Tip	.93	12.71	.80	15.89	1.39	17.67	112.29	35.16
Finish Edges	3.06							
Inspect	4.48							
Thermal Cycle	.43							
Zyglo	.32	3.90	.95	4.11	1.11	4.33	122.31	10.02
Finish Airfoil	2.28							
Inspect	.87							
Coating (O.D.)		47.42	1.00	47.42	1.05	49.79	169.73	47.42
Final Acceptance Tests		5.75	.95	6.05	1.05	6.05	184.71	14.98
TOTALS		100.00				184.67		184.71

TABLE VIII

Relative Manufacturing Costs for DSE (γ-γ'+α) Alloy Blades

Manufacturing Steps	Normalized Costs @ 100% Yields		Yield Factor	Process Cost at the Yield	Number of Operations Required	Actual Step Costs Per Part	Cumulative Value	Added Value of Step
	Individual Elements	Coupled Processes						
Fabrication								
Prepare Pattern	24.47	24.47	.80	30.59	5.93	145.11	30.59	30.57
Prepare Mold	1.57	1.57	.95	1.65	4.75	7.76	33.85	3.26
Master Melt & Revert	5.16	5.16	1.00	5.16	2.71	13.98	39.01	5.16
Cast	54.86	54.86	.60	91.43	4.51	247.42	153.01	114.00
Trim	.50							
Grind Gate	1.28	4.84	.80	6.05	2.71	13.12	197.31	44.30
Remove Core	.42							
Inspect	2.64							
Polish	5.99							
Heat Treat	.23	7.17	.80	8.96	2.16	15.49	256.60	59.29
Inspect	.95							
Acceptance Eval.	4.30	4.30	.80	5.38	1.73	7.44	324.22	68.28
Machining and Finishing								
Cast in Matrix	1.78							
Grind Root	4.19							
Grind Tip	2.55	16.06	.80	20.08	1.39	22.32	426.17	101.29
Finish Edges	3.06							
Inspect	4.48							
Thermal Cycle	.43							
Zyglo	.32							
Finish Airfoil	2.28	3.90	.95	4.10	1.11	4.33	452.70	26.53
Inspect	.87							
Coating (ID and OD)		66.39	1.00	66.39	1.05	69.71	519.09	66.39
Final Acceptance Tests		5.75	.95	6.05	1.05	6.05	552.46	33.37
TOTALS		194.77				552.73		552.46

TABLE IX

Relative Manufacturing Costs for ODSS Blades

Manufacturing Steps	Normalized Cost @ 100% Yield							
	Individual Elements	Coupled Processes	Yield Factor	Process Cost at the Yield	Number of Operations Required	Actual Step Costs Per Part	Cumulative Value	Added Value of Step
Fabrication								
Raw Material	17.50							
Fabricate Preform	.95							
Forge	1.15	20.26	.90	22.51	2.02	40.93	22.51	22.51
Inspect	.66							
Machine Blade	1.86							
ECM Passages	6.31	9.02	.95	9.49	1.82	16.42	33.19	10.68
Inspect	.85							
Coat ID	18.97							
Root Exert	4.37							
Cooling Tube	17.50	45.74	.80	57.18	1.73	79.13	98.66	65.47
Assembly	3.05							
Inspection-Acceptance	1.85							
Machining and Finishing								
Cast in Matrix	1.78							
Grind Root	1.72							
Grind Tip	.93	11.97	.80	14.96	1.39	16.64	132.29	36.93
Finish Edges	3.06							
Inspect	4.48							
Thermal Cycle	.43							
Zyglo	.32							
Finish Airfoil	2.28	3.90	.95	4.11	1.11	4.33	149.68	11.39
Inspect	.87							
Coating								
External Coat		47.42	1.00	47.42	1.05	49.79	197.10	47.42
Final Acceptance								
Tests		5.75	.95	6.05	1.05	6.05	213.29	16.42
TOTAL		144.06				213.29		213.29

TABLE X

Relative Manufacturing Costs for FRS Blades

Manufacturing Step	Normalized Costs @ 100% Individual Elements	Coupled Processes	Yield Factor	Process Cost at the Yield	Number Operations Required	Actual Step Costs Per Part	Cumulative Value	Added Value of Step
Fabrication								
Powder	2.55	2.55	1.00	2.55	2.40	6.11	3.67	3.67
Roll Powder Cloth	.70	.95	.85	1.12	2.82	2.68		
Inspect	.25							
Fibers	10.95							
Prepare Mat	.94	12.14	.85	14.28	2.82	34.22	14.28	14.28
Inspect	.25							
Press Monotape	1.68	2.27	.85	2.67	2.40	5.44	23.79	5.84
Inspect	.59							
Stamp Plies	.64							
Core Insert	2.62							
Assemble & Press	8.93	18.34	.85	21.58	2.04	37.36	49.56	25.77
Machine Airfoil	3.74							
Inspect	2.41							
Root Exert	4.37							
Cooling Tube	17.50	26.77	.80	33.46	1.73	46.35	95.42	45.86
Assembly	3.05							
Inspection Acceptance	1.85							
Machining and Finishing								
Cast in Matrix	1.78							
Grind Root	1.72							
Grind Tip	.93	11.97	.80	14.96	1.39	16.58	134.23	38.81
Finish Edges	3.06							
Inspect	4.48							
Thermal Cycle	.43							
Zyglo	.32	3.90	.95	4.11	1.11	4.32	145.40	11.17
Finish Airfoil	2.28							
Inspect	.87							
Final Acceptance Tests		5.75	.95	6.05	1.05	6.05	159.11	13.71
TOTALS		84.64				159.11		159.11

Column 4 - Process Cost at the Yield - The influence of the corresponding yield factors on the relative costs of a process are tabulated in this column. The costs are calculated by dividing the data in column two by the corresponding data from column three. Therefore, the relative costs here represent the costs incurred to produce one acceptable part by the process involved, independent of any preceding or succeeding operation. Again this latter point is significant when total manufacturing costs are later determined.

Column 5 - Number of Operations Required - The data contained in this column reflect the number of times a particular operation must be performed at its point in the manufacturing sequence to yield one acceptable finished turbine blade. The number is derived by compounding all yield factors between this process step and the final operation in the sequence. A detailed explanation of this concept is presented in the Appendix. A simplified example can be provided by considering a two-step manufacturing sequence in which each step has a 0.50 yield factor. Thus, the first operation must be performed four times to yield one acceptable finished part. Hence, the number required for step 1 becomes 4.0. These data therefore reflect the influence of compounded yield factor effects for the entire process sequence.

Column 6 - Actual Step Costs per Part - The compounding effect of yield factors on relative costs for each process/inspection sequence described in the previous column was utilized to develop the data shown in this column. The relative cost data were calculated by multiplying the costs of an operation at 100% yield (column 1) by the corresponding factor tabulated in Column 5. The resulting cost index reflects not only the discrete process step yield/factor, but the influence of compounded yield effects due to fallout occurring downstream in the manufacturing sequence.

Column 7 - Cummulative Value - These data illustrate the relative value of a component at each step in the manufacturing sequence and reflect the economic consequences of losing a part at a given point in the sequence. Equation (63) in the Appendix was utilized to determine cummulative values

Column 8 - Added Value of Step - The last column tabulates the relative value added to the part or a consequence of performing a given process step. Thus an index is provided to measure the relative importance of each process step in the manufacturing sequence. These data are obtained simply by subtracting the $i-1^{th}$ part value from the i^{th} part value to define the value added for the i^{th} step (from column 6).

It should again be emphasized that the relative cost data presented in Tables VI-I through X have been normalized with respect to costs for the DS process at 100% yield. Introduction of any further normalization within these tables would overly complicate the data presentation and make cross-comparisons particularly difficult.

An initial overview of the cost analysis will first be provided prior to a more comprehensive discussion of individual details within the various process blocks. Relative manufacturing block costs were obtained by summing the individual elemental costs within each block using costs derived for compounded yield effects. These data were then renormalized with respect to the DS system and thus represent a comparison of estimated relative manufacturing costs. The resulting estimated costs are presented in Table XI and were also utilized to construct the bar chart representative illustrated in Figure 10.

TABLE XI

Relative Manufacturing Costs for the Major Process Elements, Renormalized and Including Assumed Yield Factors

System	Fabrication	Machining and Finishing	Coating	Final Acceptance	Totals
DS	58(58%)*	12(12%)	27(27%)	3(3%)	100
DSE	243(81%)	14(5%)	38(13%)	3(1%)	298
ODSS	56(49%)	11(10%)	45(39%)**	3(3%)	115
FRS	71(83%)	12(14%)	-0-	3(3%)	86

* The figures in parentheses are percentages of the total manufacturing costs for each material/process system.

** Includes internal coating costs incurred in Fabrication sequence.

The most important, but not unexpected, observation made from the data shown in Table XI is that except for the ODSS system, fabrication costs are higher for the high technology material/process systems than for the baseline DS system. The fabrication costs are slightly more than four times greater for the DSE system compared to the DS system. The ODSS system's fabrication cost is almost identical to the DS, while the FRS system incurs only a 22% cost penalty. With regard to the Machining and Finishing column of Table XI, the slight differences in finishing costs reflect minor parameter variations in grinder operations due to different grinding characteristics. Hence Machining and Finishing represents a significant cost center but without major differences between the four systems of blade manufacture. The apparent increase in coating costs for the DSE and ODSS system shown in Table XI, reflects primarily the additional internal surface coating requirement while the baseline DS system requires only external coating and the FRS system has no coating requirements. The apparent difference in coating costs for the DSE (38) and the ODSS (45) systems reflects the influence of compounded yield factors. Although both systems utilize identical internal and external coating processes with the same corresponding discrete process yield factors, the ODSS blade has the internal coating applied earlier during the fabrication sequence. This requires that more internal coating operations be performed to produce one acceptable finished blade at the end of the process. Thus, the relative internal coating costs of 18.97 at 100% yield becomes 32.82 for the ODSS system (column 1 times column 5) and 19.92 for the DSE system.

The inherently high oxidation resistance of the matrix alloy used in the FRS system was assumed to not require a coating and hence this advantage tends to sharply offset the fabrication cost penalty of 22% over that for the DS system. Since the Final Acceptance operations are the same for all four of the material process systems, their respective costs in Table XII are identical.

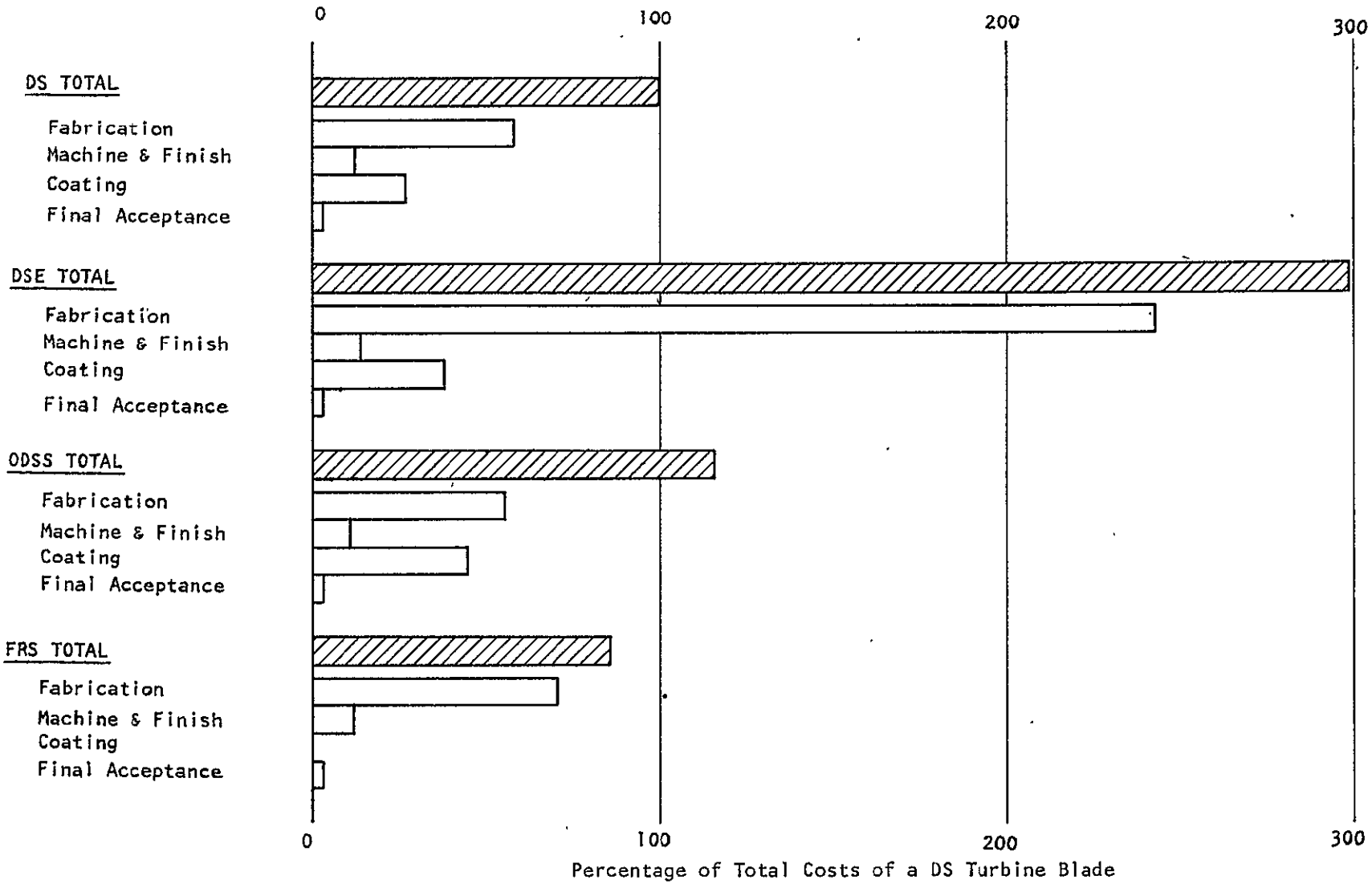

Figure 10. Relative Manufacturing Costs determined for each of the four Materials/Process Systems with assumed process yield factors.

The next step in the manufacturing cost analysis involved a more detailed examination of the individual process sequences. Major emphasis has been placed on both the Fabrication and Coating procedures.

The apparently large cost disparity between fabrication costs for DS and DSE blades are inherent in the more stringent requirements for successful investment casting of the eutectic alloy. From Column 5 of Tables VII and VIII, it is noted that patern preparation and casting incur significant cost increases for the DSE system. The requirement of the DSE casting process for maintaining an exceedingly steep temperature gradient, use of more refractory core inserts to form the hollow airfoil, and the extensions for proper growth control cause operational costs to escalate from the 45.72 index to the 145.11 level for the DSE system. The higher casting costs for DSE blades (247.42 versus 16.33) reflect primarily the relatively small number of blades per cluster in a mold assembly, e.g. 4 versus 19 for the DS process. This amounts to 1.7 blades per operator-hour in DSE and 19 in the case of DS, more than a tenfold difference. The additional controls over the solidification process for DSE castings provides the remaining cost differential. The slow withdrawal rate for DSE casting does not impact costs as greatly as would be anticipated. The reason lies in the observation that one operator can monitor three DSE furnaces at a withdrawal rate of 6.3mm/hr ($\frac{1}{4}$ inch-hr^{-1}) while doubling this rate then requires two operators to effectively monitor controls on the same three DSE furnaces. Thus, a doubling of the production rate is essentially offset by the doubled labor costs involved. There is also a slight difference in trim and core extraction costs. The greater sensitivity of the DSE alloy to crack initiation influences the sprue, gate, and riser removal processes while the internal core is required to have greater refractory properties, and as such, is also more difficult to remove following blade solidification.

Another area which had a relatively minor impact on costs involves the crack sensitivity of the DSE alloy. The least agressive metal removal parameters must be utilized in root area form grinding in the case of the DSE process blade. The DS part has an intermediate sensitivity and the equi-axed superalloy root exerts used in both the ODSS and the FRS blades exhibit the least sensitivity towards grinding-related damage. The Machining and Finishing costs reflect this defect sensitivity constraint with relative grinding cost indices of 22.32, 17.67 and 16.64 for the DSE, DS, and ODSS/FRS systems respectively.

In the case of coatings, a CoCrAlY-type overlay coating was assumed to be applied to the external surfaces of the DS, DSE, and ODSS blades. The normalized relative application costs were assumed to be the same for all three systems. An internal coating was also considered necessary for the DSE and ODSS systems which required an additional relative cost element for these systems. Recall from the initial overview discussion that external and internal coatings are sequentially applied to the DSE blade while several intermediate processing operations are conducted between internal and external coating of the ODSS blade.

One final significant point regarding the coating analysis involves the fact that these figures represent quotations for large quantity production runs from vendors of the proprietary coating systems.

The costs, therefore reflect the influence of in-process yield effects and a markup factor of undefined magnitude. All other cost elements reflect only manufacturing costs and the impact of corresponding yield factors without any markup. Thus, the estimated coating costs are unavoidably higher in relation to other elemental cost estimates. A system of equations has been provided in the Appendix to determine relative coating costs should this information become available.

4.2 Cost Driver Identification

The data of the preceding section were then analysed to extract major process cost drivers for each materials/process system. An arbitrary factor of 10% of total costs was employed to examine each materials/process system to identify those operations exceeding this level. The results of this analysis are summarized in Table XII.

TABLE XII

Process Operations Exceeding 10% of Total Cost

(with Assumed Yield Factors)

Material/Process System	Operation	Relative Cost	% of Total Cost of Mfg.	
DS	Prepare Pattern	45.72	25	
	Post-Fab Metal Removal	17.67	10	62%
	Coating	49.79	27	
DSE (γ-γ'+α)	Prepare Pattern	145.11	26	
	Casting	247.42	45	84%
	Coating	69.71	13	
ODSS	Raw Material & Forge	40.39	19	
	Root Assembly	79.13	37	79%
	Coating	49.79	23	
FRS	W Fibers & Collimation	34.22	22	
	Ply Stamp and Assembly	37.36	23	84%
	Root Exert and Assemble	46.35	29	
	Root Grinding	16.58	10	

Efforts to reduce costs in any of the candidate materials/process systems should be directed to the operations identified in Table XII. One major observation that can be made concerns the overall cost driver situation. This observation relates to the totalized percentages listed in the extreme right-hand column of Table XII. The major cost drivers for the mature DS manufacturing sequence amount to only 62% of total manufacturing costs which the major cost drivers for high technology systems comprise approximately 80 to 85% of total costs. A reasonable assumption therefore appears to be that successful technological maturation of the advanced blade systems would effect cost reductions in these critical areas and provide a cost partition between major and minor cost drivers comparable to those defined for the baseline DS system.

It is recognized that the assumption represents an overall generalization, but the basic point is that mature manufacturing operations have, in fact, experienced a number of cost reduction cycles. The major cost drivers have been the subject of considerable attention as a result of this activity and normally do not comprise 80 to 85% of total manufacturing costs.

4.3 Implications of Results

The preceding analysis developed considerable insight into the processing details and associated cost factors for the three candidate high technology blade material/process systems.

One of the most interesting implications involves the DSE materials/process system. The major cost drivers for DSE parts are the mold preparation and casting operations. Development of the necessary technology for maintaining the steep thermal gradient for mold clusters containing the same number of blades as the DS system would have a significant impact on casting costs. There are two possible techniques to achieve this goal. The first would involve casting an airfoil shape and thus eliminate the structure control problems associated with the relatively large sectional changes at the airfoil/platform transition. A root exert cast of an equiaxed superalloy could then be attached by braze diffusion bonding in the manner proposed for the ODSS and FRS systems. This approach would also avoid the shear strength limitations inherent in root attachment designs for the DSE material. An alternative method would be to cast a monolithic shape and electrochemically machine (ECM) the airfoil geometry to net shape and provide a near-net root serration configuration. Both approaches would provide significant process cost reductions, including the following:

1. Mold and pattern preparation costs would be reduced,
2. Withdrawal rates could be increased,
3. less eutectic alloy would be required to cast airfoils by the former technique, and
4. mold and metal reactions would be relatively unimportant for the latter technique.

Successful efforts in these areas could reduce manufacturing costs for DSE systems to the point where they are competitive with the other two high technology systems.

The major cost center for the ODSS and FRS materials/process systems is the root exert and assembly operation. In the case of ODSS, a possible solution to this problem might be a bi-casting process in which the root exert would be cast in place directly on the net forged airfoil. This would eliminate the need to machine the lower portion of the airfoil to accept the exert and would also reduce assembly costs. The high temperatures involved might not seriously degrade the ODSS properties, but it would most likely not be feasible for the FRS system.

In the case of FRS, alternative procedures for making root attachments include new net-shape isothermal forging in which root plies are bonded to form a finished root shape in the same operation as bonding of the airfoil.

The coating process required for both the DSE and ODSS systems also represents a major cost center. Alternatives to the external overlay coating could include cladding the airfoil with a sheet of FeCrAly material by a hot-pressing operation. This operation could also be utilized to attach the root exert and impact net airfoil/near-net root geometries by utilizing the emerging isothermal forging technology. This alternative offers a solution to fundamental problems inherent in both the DSE and ODSS high technology materials/process systems. A simplified manufacturing sequence for each system would then contain the following basic steps:

DSE

1. Cast airfoil and ECM undersize
2. Layup cladding and root structures of appropriate sheet materials
3. Hot press to consolidate and attain a net airfoil
4. Remove core
5. Machine root
6. Coat internal surface

ODSS

1. Directionally forge airfoil
2. Same as #2 in DSE
3. Same as #3 in DSE
4. ECM internal passages
5. Same as #6 in DSE
6. Install cooling tube
7. Machine Root

One very critical point which was discussed previously and will again be re-emphasized is that the relative cost levels between the candidate systems can be extremely sensitive to blade design. Turbine blades having roots offset with respect to the airfoil and/or relatively large trailing edge overhang are a major problem to manufacture by the FRS system and very difficult using the ODSS system. Design of a curved root attachment would restore process feasibility if this design alternative is included in the analysis. Failure to include a measure of design freedom in the evaluation of these advanced turbine blade systems can lead to serious errors or biased comparisons.

A final implication of this work is that the cost models generated provide the basic framework for developing similar comparisons of other blade designs on manufacturing methods. One particular application would be a study of the use of the thermal barrier coating[7] on equi-axed blade coatings as a direct competitor to the high-technology material/process systems analyzed during this program. Basically this approach seeks to limit metal temperatures with a barrier rather than developing alloy systems having useful mechanical properties at metal temperatures of 1100-1200°C (2012 to 2192°F).

5.0 REFERENCES

1. Moracz, D. J., "Investigate Feasibility of Near Net Vane Shape Processes in Advanced Oxide Dispersion Strengthened (ODS) Alloys", General Electric Subcontract under NAS3-19710, July 1976.

2. Perkins, R. J. and Bailey, P.G., "Low Cost Processes for Manufacture of Oxide Dispersion Strengthened (ODS) Turbine Nozzle Components", Contract No. F33615-76-C-5235, Interim Technical Report No. 3, 1 January 1977 - 31 March 1977.

3. R. H. Barkalow, et.al., "The Mechanical Properties of the Directionally Solidified $\gamma/\gamma'-\delta$ Eutectic Alloy", p. 549 of "Conference on In Situ Composites - II", edited by M. R. Jackson et.al; Xerox Individualized Publishing, 1976.

4. K. D. Sheffler and J. J. Jackson, "Stress Analysis, Thermomechanical Fatigue Evaluation, and Root Subcomponent Testing of Gamma/Gamma Prime-Delta Eutectic Alloy", NASA CR-135005, December 1976.

5. Brentnall, W. D., "Metal Matrix Composites for High Temperature Turbine Blades", NADC 76225-30, April 1976.

6. Brentnall, W. D. and Moracz, D. J., "Tungsten Wire-Nickel Base Alloy Composite Development", NASA CR-135021, March 1976.

7. Levine, S. R. and Clark, J. S., "Thermal Barrier Coatings - A Near-Term High-Payoff Technology", NASA-TMX-73586, January 1977.

6.0 APPENDIX

The Appendix contains a discussion of the logic behind the cost model equations utilized to calculate the relative manufacturing costs and presents the resulting equations. A glossary of terms is also provided to define the various factors comprising these equations. The sections are organized according to the flow charts previously presented. Each of the Fabrication processes are treated individually and the succeeding Machining and Finishing, Coating, and Final Acceptance Tests are treated collectively for all candidate systems. The rationale for collective treatment can be justified by the fact that blades emerging from any of the four Fabrication procedures have virtually an identical external physical appearance. The same finishing procedures are used for all systems with the only differences being in the specific grinding or coating parameters necessary for each system.

The most general equation which describes the costs associated with a manufacturing process is:

$$K = \frac{LOH}{nm} (\Sigma t) + C$$

where: K = cost per part of the process

LOH = labor and overhead rate

n = number of parts per batch

m = number of batch processes operated simultaneously by one operator

t = time required to complete one task for the batch

C = raw material costs for one part

When applying this model to the various manufacturing steps for the three candidate systems and the baseline conventional DS method, equations specific to the requirement were developed. The models were developed only to the detailed extent justified by the reliability of the input data available. Hence, in many cases, trivial costs were absorbed as part of the overhead rate estimate. It was anticipated that this assumption was valid because it was uniformly applied to all systems and the total impact on relative costs was negligible. Equipment use and tooling consumption costs have also been included in the overhead burden, a common industry practice.

6.1 Fabrication Cost Model

Three basic fabrication models were developed for the candidate high technology blade manufacturing materials/process systems. The fabrication sequences for the directionally solidified (DS) system used for the baseline data and the directionally solidified eutectic (DSE) system utilized a common series of process elements; hence, these can be described by the same general

model. Differences in input data to the models develop the distinctions between the two systems. The oxide dispersion strengthened superalloys (ODSS) and fiber reinforced superalloy (FRS) systems required development of two additional fabrication models.

6.1.1 DS/DSE Fabrication Models

The flow chart developed for the Fabrication sequence is presented in Figure A-1. The first step in the DS/DSE casting process is the preparation of a cluster of wax patterns that will be invested. The steps involved in the cluster manufacture are: the wax injection of the patterns with internal cores and other mold components, the assembly of the various mold parts, dressing of the cluster assembly, and an inspection of the finished cluster. The equations for the cost model for these steps is given by:

$$K_{pp} = \left(\frac{1}{n_c}\right) \left[LOH(t_{amp} + t_{dc} + t_{ci}) + K_{cl}\right] + K_p \qquad (1)$$

where: K_{pp} = cost of pattern preparation
n_c = number of blades per cluster
t_{amp} = time to assemble the patterns in a cluster
t_{dc} = time required to dress the cluster
t_{ci} = time required to inspect the cluster
K_{cl} = cost of cluster components other than the pattern
K_p = cost of a wax pattern

The costs of both the cluster parts and the pattern were further resolved as:

$$K_{cl} = LOH\ (t_{imp}) + C_w\ W_{wmp} \qquad (2)$$

where: C_w = wax cost on a weight basis
W_{wmp} = weight of wax for mold parts
t_{imp} = injection time

and;

$$K_p = LOH\ (t_{dic} + t_{ip} + t_{ifp}) + C_w\ W_{wp} + C_k \qquad (3)$$

where: t_{dic} = time to dress and inspect the cores
t_{ip} = time required to inject the pattern
t_{ifp} = time required to inspect final pattern
W_{wp} = wax weight in the pattern
C_k = raw core cost

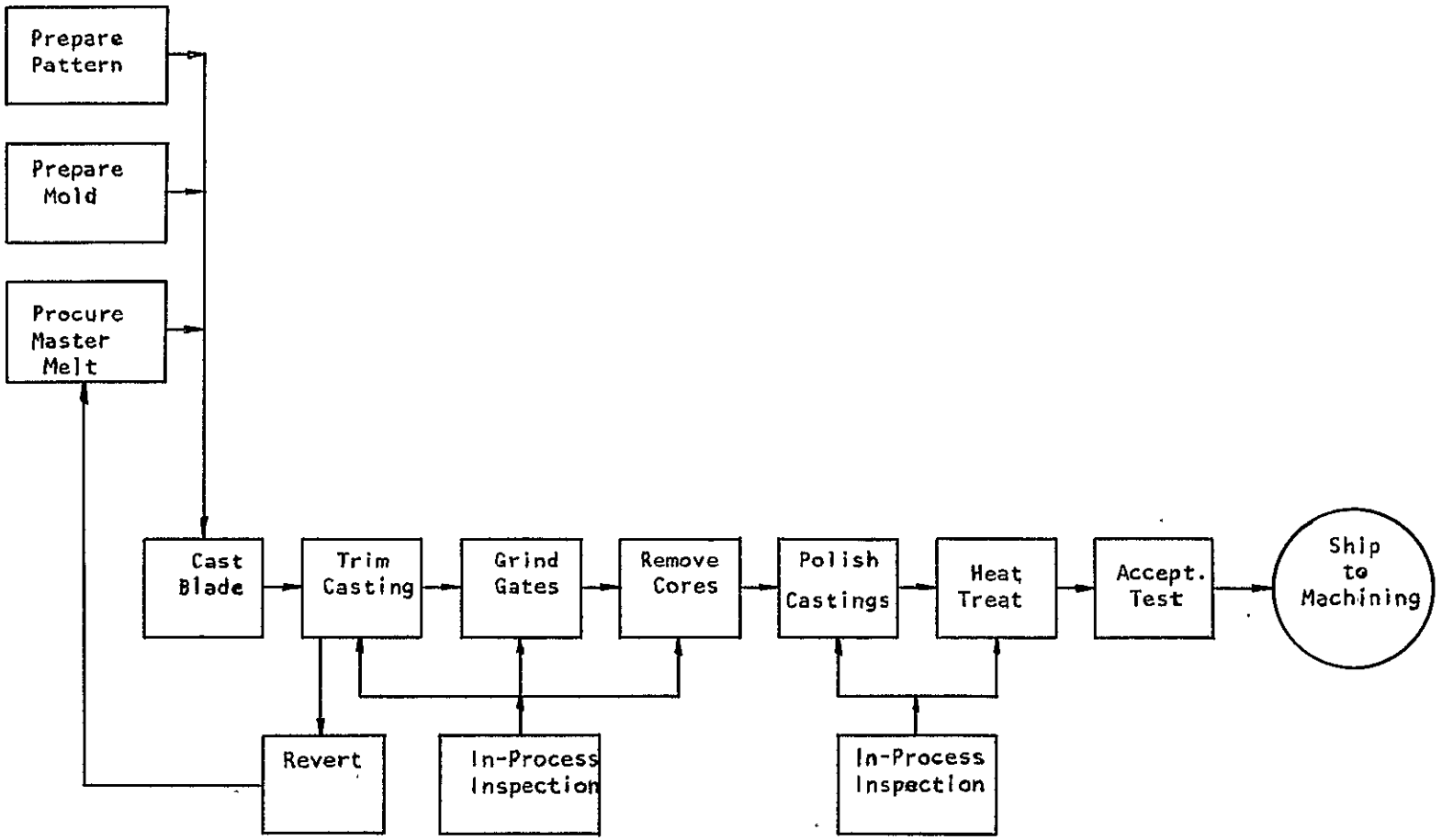

Figure A1 Fabrication Sequence for DS and DSE Turbine Blades.

After the cluster of wax patterns is complete, it is invested by successive dips in ceramic slurries to form the refractory mold structure. This step corresponds to the second operation on the DS/DSE flow chart. The ceramic is then dehumidified, the wax pattern melted out, and the major portion of the wax recovered. The green mold is then fired (to burn off any residual wax), cleaned and inspected. The cost model equation for this block is:

$$K_{pm} = \frac{1}{n_c} \left(LOH(t_{dd} + t_{dcc} + t_{mw} + t_{fci}) + W_{cer}\, C_{cer} - W_{wr}\, C_w\right) \qquad (4)$$

where: K_{pm} = cost of mold preparation
t_{dd} = time required to dip and dry investment mold
t_{dcc} = time required to dehumidify the ceramic
t_{mw} = time required to melt out the wax
t_{fci} = time required to fire, clean and inspect
W_{cer} = weight of the ceramic
C_{cer} = weight cost of the ceramic
W_{wr} = weight of the wax revert

The casting process follows mold firing. The major cost element of this operation is the basic raw material cost and can be defined as:

$$K_{mm} = \frac{1}{n_c} \left(C_m\, (W_m - W_{mr})\right) \qquad (5)$$

where: K_{mm} = cost of master melt
n_c = number of blades per cluster
C_m = weight cost of the metal
W_m = amount of metal in a pour
W_{mr} = revert weight

The labor cost during the casting operation involves two factors. One factor is the sum of the constant costs of cleaning, set-up, preheating, pouring, removing the mold from the furnace and removing the ceramic. The other factor is the labor costs associated with the prevailing withdrawal velocity of the mold from the furnace. The cost model for the entire casting operation is:

$$K_c = \frac{1}{n_c m_f} \left(LOH\, (t_{ct} + \frac{1}{v})\right) \qquad (6)$$

where: K_c = casting cost

m_f = number of furnaces per operator

t_{ct} = total constant time needed to cast a batch regardless of the withdrawal rate

l = withdrawal length

v = withdrawal velocity

After the cluster is cast, the individual blades are cut off and trimmed and the alloy is reverted. The cost model is:

$$K_{tcg} = \frac{LOH}{n_c} (t_{cot}) \tag{7}$$

where: K_{tcg} = cost of trimming the casting

t_{cot} = time required for blade cut-off and trim

Note that the revert is assigned to the raw material block and not to this block where the casting is trimmed where the revert actually occurs. This was done so that no false impression of low trim costs would be made.

Next the blades are ground to remove gate and riser projections. From this step onward, the blades are now individual units. During the grinding step, the gating root is leveled off and the gate tip is removed. Also, the trailing edge flash is snagged off. The cost equation is:

$$K_g = LOH\ (t_{ggr} + t_{ggt} + t_{stf}) \tag{8}$$

where: K_g = cost of grinding flash

t_{ggr} = time to grind the gating root

t_{ggt} = time to grind the gate tip

t_{stf} = time to snag the trailing edge flash

After grinding the core is removed by vaporization in an autoclave. A large batch can be processed simultaneously. The cost of removing the core is:

$$K_{rc} = \frac{LOH}{n_a} (t_{rc}) \tag{9}$$

where: K_{rc} = core removal costs

n_a = number of blades per autoclave batch

t_{rc} = autoclave cycle time

After the core is removed, an inspection is made to ensure that the core is entirely removed and that the wall thickness is correct. The alloy type

and grain size are also characterized. The costs for these inspection steps are merely the time requirements multiplied by the labor and overhead rate:

$$K_{ip1} = LOH\ (t_{crc} + t_{cwt} + t_{cat} + t_{cgs}) \tag{10}$$

where: K_{ip1} = cost of first in-process inspection
t_{crc} = core removal inspection time
t_{cwt} = wall thickness inspection time
t_{cat} = alloy type inspection time
t_{cgs} = grain size inspection time

The approved castings are now polished. The whole blade is polished and blended, buffed and finally blasted. The costs are:

$$K_{pb} = LOH\ (t_{pt} + t_{bdt} + t_{but} + t_{blt}) \tag{11}$$

where: K_{pb} = blade polish costs
t_{pt} = polish time
t_{bdt} = blend time
t_{but} = buff time
t_{blt} = blast time

The blade is heat treated to relieve stresses. This involves a timed cycle in a protective atmosphere furnace. The resulting costs are defined by:

$$K_{ht} = \frac{LOH}{n_f}\ (t_{ctf}) \tag{12}$$

where: K_{ht} = cost of heat treatment
n_f = number in a cycle
t_{ctf} = cycle time of the heat treatment

Another in-process inspection follows heat treatment. Here the blade is checked for possible defects by the zyglo process, and it undergoes both a visual and dimensional examination. The cost for these inspections are:

$$K_{ip2} = LOH\ (t_{zy} + T_{vis} + t_{dim}) \tag{13}$$

where: K_{ip2} = second in-process inspection cost
t_{zy} = time for zyglo
t_{vis} = visual checking time
t_{dim} = dimensional checking time

The acceptance testing follows the preceding in-process inspection, and it is basically a sequence of final preparations for characterizing the casting as a complete unit. The inspections include another dimensional check, a wall thickness check, an airflow check, a final X-ray, a visual inspection of the core passages, and an alloy check. The costs are:

$$K_{fai} = LOH\ (t_{dmf} + t_{wtf} + t_{vcf} + t_{acf}). \tag{14}$$

where: K_{fai} = cost for final acceptance
t_{dmf} = time for dimensional check
t_{wtf} = time for wall thickness check
t_{vcf} = time for visual core examination
t_{acf} = time for alloy check

The total cost for the DS or DSE fabrication process is the sum of the block costs; if there is no fallout:

$$K_{DS/DSE} = K_{pp} + K_{pm} + K_{mm} + K_c + K_{tcg} + K_g + K_{rc} + K_{ipl} + K_{pb} + K_{ht} + K_{ip2} + K_{fai} \tag{15}$$

The impact of yields on the process will be treated as a separate item and is described in Section 6. The completed parts are now ready for the machining and finishing process sequence.

6.1.2 ODSS Fabrication Model

Cost models for ODSS fabrication were developed for each manufacturing block defined by the flow chart presented in Figure A2.

The first block represents the raw material input for the preform. The cost of the preform material will be:

$$K_{rm} = W_p\ (C_{brs}) \tag{16}$$

where: K_{rm} = raw material cost (bar stock)
W_p = weight of the preform
C_{brs} = cost of ODSS bar stock on a weight basis

The second block represents the operations required to make the preform. The cost model is:

$$K_{fp} = LOH\ (t_{cop} + t_{dp}) \tag{17}$$

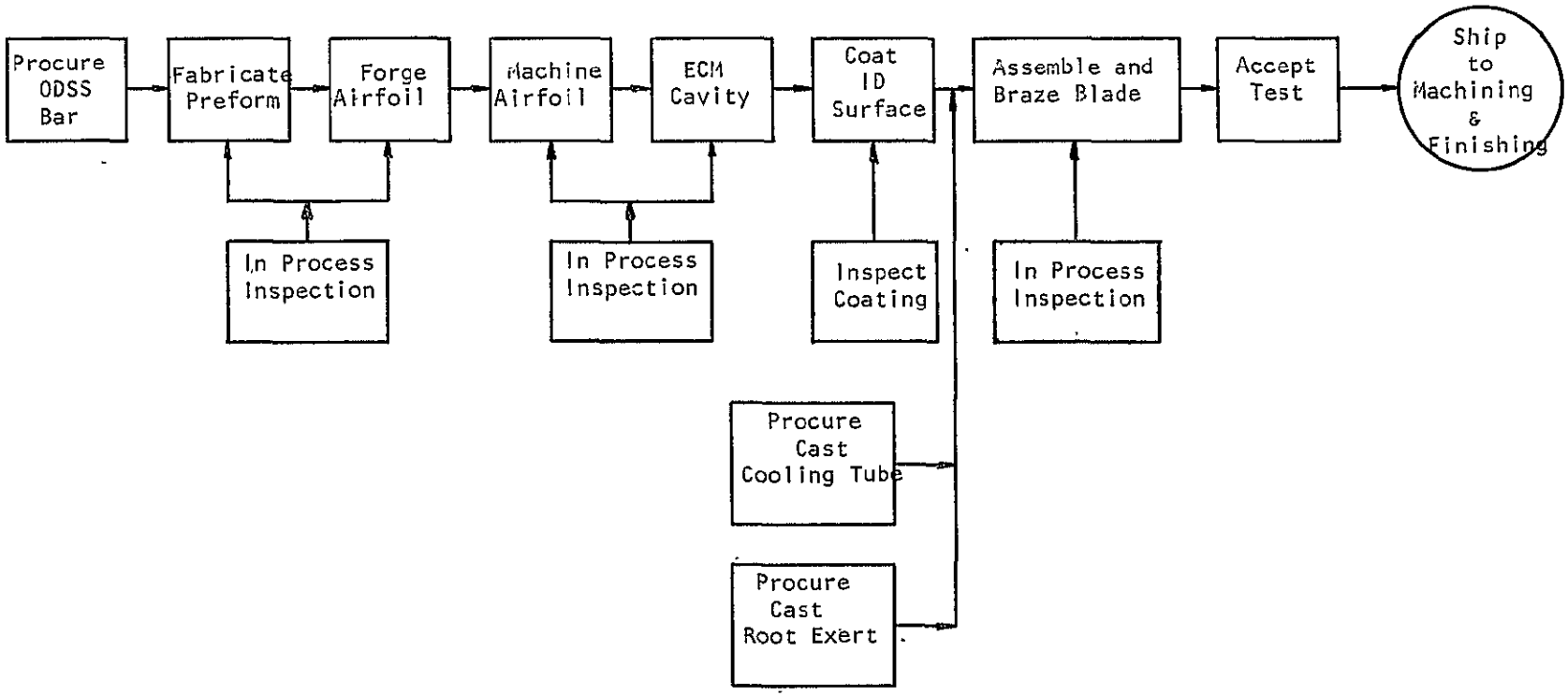

Figure A2 Fabrication Sequence for ODSS Turbine Blades

where: K_{fp} = preform fabrication costs

t_{cop} = the time required to cut-off and label one preform

t_{dp} = the time required to deburr one preform

The third block indicates the forging operation. The preform is coated with lubricant, forged, descaled and then deburred. The corresponding cost model is:

$$K_{fg} = LOH\ (t_{cd} + t_{hf} + t_{ds} + t_{dbr}) \tag{18}$$

where: K_{fg} = forging costs

t_{cd} = coating time for lubricant

t_{hf} = heat and forge time

t_{ds} = time for descaling

t_{dbr} = time for deburring

The fourth block is an in-process inspection block. Here the forging undergoes a visual inspection for flaws, a dimensional check, and an alloy compositional check. The cost model for this step is:

$$K_{in1} = LOH\ (t_{ve} + t_{dif}) + \frac{C_{mcl}}{n_{mcl}} \tag{19}$$

where: K_{in1} = first inspection cost

t_{ve} = time required for a visual examination

t_{dif} = time required for the dimensional inspection

C_{mcl} = cost to check a batch of forgings for composition

n_{mcl} = number in the batch

The fifth block is for the machining operation. Here the raw forging of the airfoil is ground to length, the bottom of the airfoil is machined to a taper to accept the root, and the leading and trailing edges (L&TE) are blended. The cost model is:

$$K_{mac} = LOH\ (t_{gtl} + t_{mfr} + t_{be}) \tag{20}$$

where: K_{mac} = machining costs

t_{gtl} = time required to grind the airfoil to length

t_{mfr} = time required to machine the airfoil for the root

t_{be} = time required to blend the L&TE of the airfoil

The sixth block corresponds to the Electro-Chemical Machining (ECM) of the internal airfoil cavity. A slot is machined through the center of the airfoil, and the trailing edge (TE) holes are also made by ECM. The cost model for this process is:

$$K_{ecm} = LOH \left(\frac{l_1}{n_1 m_1 v_1} + \frac{l_2}{n_2 m_2 v_2} \right) \quad (21)$$

where: K_{ecm} = cost of ECM
l_1 = length of the center cavity
n_1 = number of airfoils machined in one set-up for ECM of cavity
m_1 = number of machines per operator for ECM of cavity
v_1 = linear velocity of ECM electrode during cavity machining
l_2 = machining length of the TE holes
n_2 = number of airfoils in one machine cycle for ECM of TE holes
m_2 = number of machines per operator for ECM of TE holes
v_2 = velocity of ECM electrode during ECM of TE holes

The seventh block represents another inspection step. The airfoil is checked for air flow and dimensions after ECM. The cost model for this inspection step is:

$$K_{ins} = LOH \ (t_{aam} + t_{dam}) \quad (22)$$

where: K_{ins} = inspection cost
t_{aam} = time for airflow check
t_{dam} = time for dimensional check

The eighth block is for application of the internal coating. The ODSS blade was assumed to be coated internally before the cooling tube is inserted, and the coating was assumed to be put on by an outside vendor. The cost model for the coating is:

$$K_{ic} = C_{ic} + LOH \ (t_{ic}) \quad (23)$$

where: K_{ic} = internal coating cost
C_{ic} = purchased price of the coating per blade
t_{ic} = time required to inspect the coating when the blade is returned

The ninth and tenth blocks represent material inputs for the root exert and cooling tube, respectively. These costs were also obtained as quotes from outside vendors. Thus:

K_{rt} = cost of root exert (24)

K_{ct} = cost of the cooling tube (25)

The eleventh block corresponds to the assembly of the cooling tube, root and airfoil. The parts are degreased, assembled, brazed and cleaned. The cost model for this process is:

$$K_{br} = LOH\ (t_{dfb} + t_{aab} + t_{cof}) \tag{26}$$

where: K_{br} = braze costs
t_{dfb} = degrease time
t_{aab} = assemble and braze time
t_{cof} = cleaning time

t_{aab} which is the assemble and braze time can be examined further. First the cooling tube is inserted and a whole batch is run through a furnace cycle. Then the root is attached by a similar process. Thus the expanded expression for t_{aab} is:

$$t_{aab} = t_{act} + \frac{t_{bct}}{n_{bct}} + \frac{t_{brt}}{n_{brt}} + t_{art} \tag{27}$$

where: t_{act} = assemble time for the cooling tube
t_{bct} = time for a braze furnace cycle for the cooling tube
n_{bct} = number of parts per furnace for the cooling tube braze cycle
t_{art} = assembly time for the root
t_{brt} = time for the total braze cycle for the root
n_{brt} = number of pieces per furnace for the root braze cycle

The twelfth block is for the final inspection. The whole assembly undergoes a visual, airflow, and dimensional examination. The cost model is:

$$K_{fia} = LOH\ (t_{vet} + t_{tfd} + t_{tfa}) \tag{28}$$

where: K_{fia} = final fabrication inspection cost
t_{vet} = visual examination time.
t_{tfd} = time for the dimensional check
t_{tfa} = time for the airflow inspection

The total cost for ODSS fabrication without considering the effect of yield factors is:

$$K_{ODSS} = K_{rm} + K_{pc} + K_{inl} + K_{mac} + K_{ins} + K_{ic} + K_{rt} + K_{ct} + K_{fia} \quad (29)$$

where the K's have been defined previously. Again, the impact of yield factors will be separately treated in Section 6. The as-fabricated ODSS blades are now ready for the Post-Fabrication operation.

6.1.3 FRS Fabrication Model

Cost models were developed for each manufacturing block illustrated in Figure A3 for FRS fabrication.

The first of two blocks defining raw material costs involves the powdered matrix alloy; the cost equation is simply:

$$K_{pow} = \frac{W_{pb} C_{pw}}{n_{pb}} \quad (30)$$

where: K_{pow} = powder cost
W_{pb} = weight of powder in a batch
C_{pw} = weight cost of metal powder
n_{pb} = number of finished turbine blades which can be made from a powder batch

The second block concerns the manufacturing step where the powder cloth is produced. Here the powder is blended, rolled, and cut into rectangular sheets. The cost model is:

$$K_s = \frac{LOH}{n_{rb}} (t_{bld} + t_{rol} + t_{cut}) \quad (31)$$

where: K_s = cost of powder cloth
t_{bld} = blend time per batch
t_{rol} = roll time per batch
t_{cut} = cut time per batch
n_{rb} = number of turbine blades per batch

The third step is an in-process inspection step. Here the cloth is inspected for thickness and density. The cost model is:

$$K_{is} = \frac{LOH}{n_{rb}} (t_{dit} + t_{thi}) \quad (32)$$

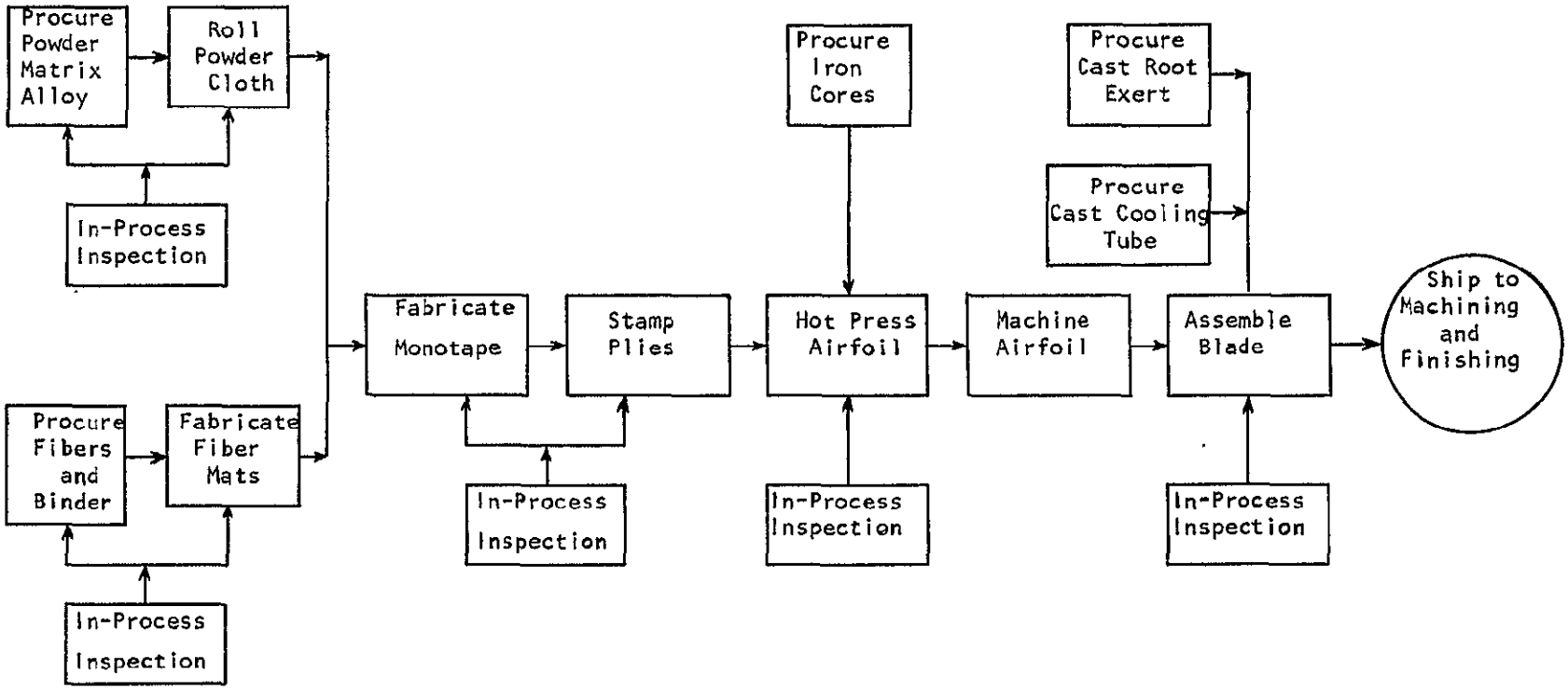

Figure A3 Fabrication Sequence for FRS Turbine Blades

where: K_{is} = cost to inspect the powder cloth
t_{dit} = density inspection time per batch
t_{thi} = thickness inspection time per batch

The fourth step is the other raw material input (i.e., fibers and binder) to the FRS manufacturing sequence. The cost is:

$$K_{fi} = \frac{W_f C_f}{n_{fb}} \tag{33}$$

where: K_{fi} = fiber cost
W_f = weight of fibers in a batch
C_f = cost by weight of the fibers
n_{fb} = number of turbine blades obtained from a batch

The fifth step is where the fibers are collimated into mats by a drum winding technique. The fibers are wrapped around a drum with a polystyrene binder, removed from the drum, and cut into sheets. The cost is:

$$K_{mat} = \frac{LOH}{n_{rm}} (t_{rft} + t_{cmt} + t_{mat}) \tag{34}$$

where: K_{mat} = mat assembly costs
n_{rm} = number of parts per batch
t_{rft} = roll time per batch
t_{cmt} = batch time required to cut the fibers into mats
t_{mat} = assembly time per batch

Next the mats are inspected visually for proper spacing. The cost is:

$$K_{im} = LOH\ (t_{rmi}) \tag{35}$$

where: K_{im} = mat inspection costs
t_{rmi} = inspection time (visual) per mat

During the seventh step in the fabrication sequence, the cloth sheets and the fiber mats are stacked and hot pressed together to form pre-consolidated monotapes. The cost model is:

$$K_{fm} = \frac{LOH}{n_m} (t_{cs} + t_{cf} + t_{aip} + t_{ltp} + t_{ep} + t_{hpt} + t_{rfp} + t_{ets}) \tag{36}$$

where: K_{fm} = monotape fabrication costs

t_{cs} = time to coat separators per pressing batch

t_{cf} = time to cut foil per pressing batch

t_{aip} = assembly time per pressing batch

t_{ltp} = time required to load the press per pressing batch

t_{ep} = time to evacuate the press per pressing batch

t_{hpt} = hot press time per pressing batch

t_{rfp} = time required to remove the monotapes from the press per pressing batch

t_{ets} = etch time for separators per pressing batch

n_m = number of blades which can be obtained from a press batch

The individual monotapes are next inspected for thickness, and the fibers are examined by X-ray to assure proper collimation. The cost model is:

$$K_{imt} = \frac{LOH}{n_{mt}} (t_{xrm} + t_{mt}) \tag{37}$$

where: K_{imt} = monotape inspection costs

n_{mt} = numbers of blades per monotape

t_{xrm} = X-ray time per monotape

t_{mt} = monotape thickness inspection time

The next step represents the stamping process, in which the individual plies are cold blanked from the consolidated monotapes. The costs are:

$$K_{stp} = \frac{LOH}{n_{mt}} (t_{st}) \tag{38}$$

where: K_{stp} = stamping cost

t_{st} = time to stamp the plies required from one monotape

Next the plies are assembled with the iron core and hot pressed to form the basic airfoil configuration. The costs for this step are:

$$K_{asf} = C_c + \frac{LOH}{m_p n_{bp}} (t_{sal} + t_{prs} + t_{up}) \tag{39}$$

where: K_{asf} = airfoil assembly cost
C_c = core cost
n_{bp} = number of blades per pressing batch
m_p = number of presses per operator
t_{sal} = stack and load time per batch
t_{prs} = press time per batch
t_{up} = unload time per batch

The next block represents the step where the airfoil is machined. Here it is blended and polished, and the iron core is removed by an acid bath. The cost equation is:

$$K_{maf} = \frac{LOH}{n_b n_{opb}} (t_b) + LOH (t_{pa} + t_{baf}) \quad (40)$$

where: K_{maf} = cost to machine the airfoil
n_b = number of blades in an acid tank
n_{opb} = number of baths per operator
t_b = time required to remove the core
t_{pa} = time required to polish the airfoil
t_{baf} = time required to blend the airfoil

The thirteenth block corresponds to an in-process inspection procedure. The airfoil is X-rayed to be certain that the core is entirely removed and no voids remain from the ply consolidation. There are also visual and dimensional inspections and an airflow check. The representative cost model is:

$$K_{iam} = LOH (t_{vam} + t_{di} + t_{xam} + t_{ai}) \quad (41)$$

where: K_{iam} = post machining inspection cost
t_{vam} = visual inspection time
t_{di} = dimensional inspection time
t_{xam} = X-ray time
t_{ai} = time for airflow check

After this inspection, a cooling tube and a cast root exert are assembled onto the airfoil, brazed, and inspected. The FRS blade is now ready to proceed to the post-fabrication sequence. The cost model for the FRS blade after the airfoil inspection is the same as the ODSS process after the step for application

of the internal coating. The costs for these later steps are also identical because the inputs to the models will be the same and are given by equations (24) through (28).

The overall cost for the FRS fabrication step is:

$$K_{frs} = K_{pow} + K_s + K_{is} + K_f + K_{mm} + K_{im} + K_{fm} + K_{imt} + K_{stp} + K_{asf} + K_{maf} + K_{iam} + K_{rt} + K_{ct} + K_{br} + K_{fia} \quad (42)$$

This cost is the cost of fabrication without fallout or recycle, or the cost of an ideal process with 100% yield.

6.2 MACHINING AND FINISHING COST MODEL

At this point of the manufacturing sequence, all blade materials/process systems are virtually identical in external appearances. The same overall manufacturing cost model can be utilized to describe post-fabrication sequences in all cases. Basically, the process sequence involves: imparting the root attachment geometry by precision form grinding; grinding the tip radius; heat treating to expose any grinding damage; and a number of in-process inspection procedures. The overall process flow chart developed for the Post-Fabrication operations is presented in Figure A4.

The first step in the Post-Fabrication sequence consists of casting the airfoil portion in a low melting matrix alloy to provide rigid support for the subsequent grinding operations. The cost model for this process is:

$$K_{cim} + LOH\ (t_{cim}) \quad (43)$$

where: K_{cim} = cost to cast blade in matrix
t_{cim} = time required to cast the blade in its matrix block

The matrix alloy is later recovered virtually 100% for re-use.

The next step is where the potted blade is precision form ground in the root area. Here the serrations, plus the leading and trailing edges of the root are ground. The part is then removed from the matrix, and the airfoil tip is ground. This cost is:

$$K_{pfg} = K_{gs} + K_{gr} + K_{tg} \quad (44)$$

where: K_{pfg} = post-fabrication grinding cost
K_{gs} = serration grind cost
K_{gr} = root grind cost
K_{tg} = tip grind cost

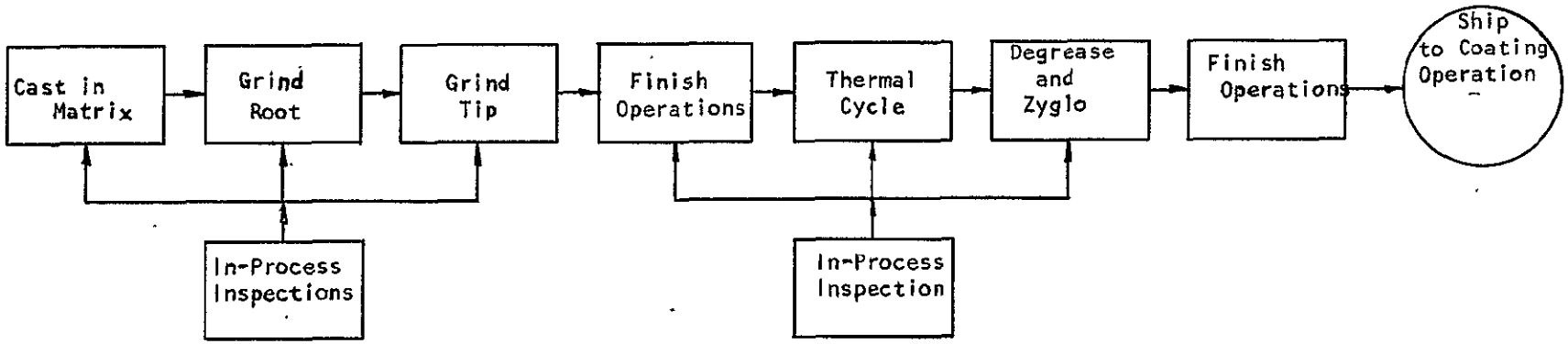

Figure A4 Process Flow Chart for the Machining and Finishing Sequence for all Fabrication Methods.

The equation describing the costs for the grinding of the serration in a batch-process is:

$$K_{gs} = \frac{LOH}{n_g} \left(\left(\frac{t_{c1} l_s}{f_{g1} v_t} + \frac{t_{c2} l_s}{f_{g2} v_t} + \frac{n_s l_s}{v_t} + t_l + t_d \right) \right) \quad (45)$$

where:
- n_g = number of blades per batch
- t_{c1} = total rough depth of cut
- l_s = stroke length
- f_{g1} = rough feed per pass
- v_t = table velocity
- t_{c2} = total finish depth of cut
- f_{g2} = finish feed per pass
- n_s = number of sparkout strokes
- t_l = load time
- t_d = dress time

The cost model for the grinding of the leading and trailing edges of the root in a batch-process is:

$$K_{gr} = \frac{LOH}{n_g} \left(\frac{t_{c2} l_s}{f_{c2} v_t} + \frac{n_s l_s}{v_t} + t_l + t_d \right) \quad (46)$$

The equation is similar to the one above, but there is no fine-grinding involved in the cycle.

The third Post-Fabrication step is the tip grind operation. The cost model for this batch-process is similar to the cost models for the other two preceding grinding steps:

$$K_{tg} = \frac{LOH}{n_g} \left(\frac{t_{c2} l_s}{f_{g2}} + \frac{n_s l_s}{v_t} + t_l \right) \quad (47)$$

After the individual turbine blades are ground, they go through some finishing operations. These include a corner break operation, slurry wash, degreasing, a core flush, and an acid soak to assure complete elimination of the matrix alloy. The cost equation for this block is:

$$K_{fop} = LOH \left(t_{pfcb} + t_{sl} + t_{pfd} + t_{cfl} + t_{as} \right) \quad (48)$$

where: K_{fop} = cost of finishing operations
t_{pfcb} = corner break time
t_{sl} = slurry time
t_{pfd} = degrease time
t_{cfl} = core flush time
t_{as} = acid soak time

The next step involves an in-process inspection. Here the root is inspected both visually and dimensionally, and an atomic absorption test is made to check on alloy composition and for residual matrix alloy contamination. The core passages are checked for alloy type and inspected visually. The cost equation is:

$$K_{pfil} = LOH\ (t_{rmv} + t_{rdi} + t_{aac} + t_{ida} + t_{cve}) \tag{49}$$

where: K_{pfil} = cost of the first machining and finishing inspection
t_{rmv} = root and matrix visual inspection time
t_{rdi} = root dimensional inspection time
t_{aac} = atomic absorption check time
t_{ida} = ID alloy check
t_{cve} = core visual examination

The next step is the thermal cycle. This process is a batch operation and can be defined as a flat rate per blade:

$$K_{tc} = \frac{\text{purchase price of the cycle}}{\text{number of blades per batch}} \tag{50}$$

After the thermal cycle, the blade is degreased and then subjected to a fluorescent penetrant (Zyglo) inspection to reveal any surface defects. The cost equation is:

$$K_{pfi2} = LOH\ (t_{db} + t_{zb}) \tag{51}$$

where: K_{pfi2} = cost of the second machining and finishing inspection
t_{db} = degreasing time
t_{zb} = zyglo time

The next to the last block in the machining and finishing sequence corresponds to a series of finishing operations. The parts are again washed and given an

acid soak and rinse cycle. The core passages are grit blasted and checked visually to assume no blockages are present. Then the part goes through a sequence of marking operations to identify alloy type, serialization, part number, etc. The representative cost model is:

$$K_{pff} = LOH\ (t_{pfw} + t_{asr} + t_{cbt} + t_{vc} + t_{mop}) \tag{52}$$

where: K_{pff} = machining and finishing final acceptance inspection costs
t_{pfw} = wash time
t_{asr} = acid soak and rinse time
t_{cbt} = core blast time
t_{vc} = visual check
t_{mop} = marking operation times

After these operations are completed, the blades are subjected to another inspection series, prior to shipment for coating. This inspection sequence consists of an airflow test, an atomic absorption inspection, and another visual inspection of the core passages and TE holes. The cost model is:

$$K_{pfa} = LOH\ (t_{pfa} + t_{paa} + t_{pri}) \tag{53}$$

where: K_{pfa} = final machining and finishing inspection cost
t_{pfa} = time for the airflow check
t_{paa} = time for atomic absorption analysis
t_{pvi} = visual inspection time for the core and the trailing edge

Blades passing the final tests are then shipped to the coating operation For 100% yield, the total cost of the post-fabrication operation is the sum of the individual block costs or:

$$K_{pf} = K_{cim} + K_{fop} + K_{pfi} + K_{tc} + K_{pfi2} + K_{pff} + K_{pfa} \tag{54}$$

The methodology used to determine the effect of yields on the process is explained in Section 6.

6.3 COATING COST MODEL

The development of a cost model for the coating operations was subject to several difficulties. The primary reason was that the high technology coating systems necessary for oxidation resistance at the higher metal temperatures are applied by proprietary processes, controlled by a limited number of vendors.

As a result, detailed process information could not be obtained. Secondly, specific coating chemistries and processes remain to be developed for the eutectic and ODSS alloy systems. Finally, it also appears that different coating systems will eventually be developed for the eutectic and ODSS alloys. It was assumed, however, that some form of overlay coating system would be applied to the exterior of the blade and a pack-deposited system used for the cooling passages.

One processing detail was obtained which pertained to process yields in that the average fallout for a coating cycle was 25%. The coating is removed from these parts, and the process is repeated. On a continuous production scale, the rejected and stripped parts are merely recycled with the following batches until all are acceptable. Thus for 100 acceptable parts; 134 coating cycles and 34 stripping cycles are required. Coating quotes from outside vendors must reflect these costs as well as an undefined markup for their proprietary process.

A series of equations has been prepared to describe the coating operation in the event detailed information becomes available in the future. These equations are valid for either external or internal overlay or vapor deposited systems. There are four basic cost centers involved: surface preparation, K_b; coating K_c; stripping, K_s; and thermal diffusion treatment, K_{ht}. Inspection operations have been incorporated as part of the clean and coat cycles. The resulting equations are as follows:

$$K_b = LOH\ (t_b + t_w + t_{ib})\ f + \frac{c_g}{n_{tg}} \tag{53}$$

where: K_b = surface preparation costs
LOH = labor + overhead rate
t_b = blast time
t_w = wash time
t_{ib} = post-blast inspection time
f = operator allowance, 1.10
c_g = abrasive grain costs per system charge
n_{tg} = number blades produced during fixture life

$$K_c = \frac{LOH}{.75}\ (t_{lu} + t_c + t_{ic})\ f + \frac{c_f}{n_{tf}} + c_m \tag{54}$$

where: K_c = coating costs
t_{lu} = load-unload time
t_c = coat time
t_{ic} = coating inspection time
c_f = coating fixturing costs

n_{tf} = number blades produced during fixture life

c_m = coating material consumed per blade

$$K_s = 0.34 \text{ LOH } (t_s) \tag{55}$$

where: K_s = strip cost

t_s = strip time

$$K_{ht} = \text{LOH } \left(\frac{t_{ht}}{n_{ht}} \right) \tag{56}$$

where: K_{ht} = thermal treatment costs

t_{ht} = heat treat cycle time

n_{ht} = parts per heat treat load

Note that the 75% yield factor has been incorporated into the coating cycle costs, K_c, and that the .34 strip cycles necessary to produce 100 acceptable parts has also been introduced into the strip costs, K_s. Total coating costs are then determined by a summation of the four elemental cost factors. In the event two coatings are required for internal and external areas, the system of equations are applied twice. Obviously, if no coatings are required, the equations are not utilized.

The data actually presented in the first volume of the series involving coating costs represent vendor coating cost quotes obtained for a pack-NiCoCrAlY and PVD-CoCrAlY coating systems. The quoted cost data were merely normalized against the remaining other cost elements to determine the relative manufacturing costs.

6.4 FINAL ACCEPTANCE COST MODEL

The final acceptance operations represent the last step in the overall turbine blade manufacturing sequence. In addition to procedures specific to this final operation, certain in-process inspection steps are repeated to insure that all parts shipped to the customer meet component specifications. These operations include shot peening of the airfoil, overall visual inspection, dimensional inspection, and application of identification numbering systems.

The equation describing this operation is:

$$K_{fa} = \text{LOH } (t_{sp} + t_{fav} + t_{fad} + t_{mar}) \tag{57}$$

where: K_{fa} = final acceptance inspection costs

LOH = labor plus overhead rate, $/min

t_{af} = airflow rate inspection time, min/blade

t_c = coating inspection time, min/blade

t_x = X-ray core time, min/blade

t_{fad} = dimensional inspection time, min/blade

t_{fav} = visual inspection time, min/blade

t_{mar} = marking time, min/blade

t_{sp} = shot peening time, min/blade

6.5 YIELD FACTOR DEVELOPMENT

The preceding descriptive cost equations have defined manufacturing costs for the Fabrication and Post-Fabrication operations without regard for accept/reject criteria or process yields. Realistic cost estimates must address this important consideration and make adjustments according to expected process yields. There are two independent approaches to examination of yield factor impact on costs. The first involves consideration of simple, or straight, yield factors for each individual process step. This concept has been identified as the "uncoupled yield factor" and is useful in examining costs for a process element independent of the other process elements. The second concept, "coupled yield factor," is more complex and has been developed to consider real manufacturing conditions existing on a production line during steady-state part throughout. One or more manufacturing steps may be followed by an inspection which then determines part acceptability. Hence, the yield factor is defined in the coupled system of one or more manufacturing steps and the ensuing inspection procedure.

6.5.1 Simple Yield Factors

As outlined above, this "uncoupled yield factor" concept involves defining the true costs to process a part through a given step independent of the preceding or following process sequence. The cost defined represents that incurred to pass one good part through the particular cycle under consideration. This relatively straightforward concept is expressed by the equation:

$$K_{ap} = \frac{K_{ip}}{Y_i} \tag{58}$$

where: K_{ap} = process cost for one acceptable part

K_{ip} = process cost for i^{th} operation at 100% yield

Y_i = yield factor for i^{th} operation

This simplistic approach is valid only when an individual process element is being examined and is not applicable in determining total part costs by summing elemental process costs.

6.5.2 Coupled Process Yield Factor Development

A more complex expression for yield factors was derived for quantitatively defining the effect of many discrete yield factors on total manufacturing costs. In real manufacturing situations, accept/reject criteria are imposed during inspection operations which are performed following one or more processing steps. Thus, a yield is defined for the combined coupled system of process and inspection steps. The inspection can produce one of three results: the part is acceptable; it is unacceptable and must be scrapped; or it is unacceptable but can be repaired and recycled. This concept is illustrated in Figure A5.

The process can be treated mathematically by defining: (a) as the fraction of acceptable parts emerging from the inspection; (b) as the fraction of scrapped parts; and (c) as the fraction of parts capable of rework repair and recycling through the process. An infinite series can then be defined to describe the total fraction of good parts produced for each part entering the coupled processing/inspection sequence. This is given by the equation:

$$a \sum_{n=o}^{\infty} c^n = \frac{a}{1-c} \tag{59}$$

where n is the number of times a part is recycled with (a) and (c) as defined previously. Similarly, the fraction of scrap parts produced per part entering the sequence is defined as:

$$b \sum_{n=o}^{\infty} c^n = \frac{b}{1-c} \tag{60}$$

and, hence, the total fraction that is recycled is:

$$\sum_{n=1}^{\infty} c^n = \left(\sum_{n=o}^{\infty} c^n\right) - 1 = \frac{c}{1-c} \tag{61}$$

The term K_i is then defined as the overall cost of the sequence to produce one part at 100% yield, the actual costs to produce parts under more realistic conditions can be defined by the following rigorous expression:

$$K_y = \frac{K_i\left(\frac{a}{1-c} + \frac{b}{1-c} + \frac{c}{1-c}\right)}{\frac{a}{1-c}} \tag{62}$$

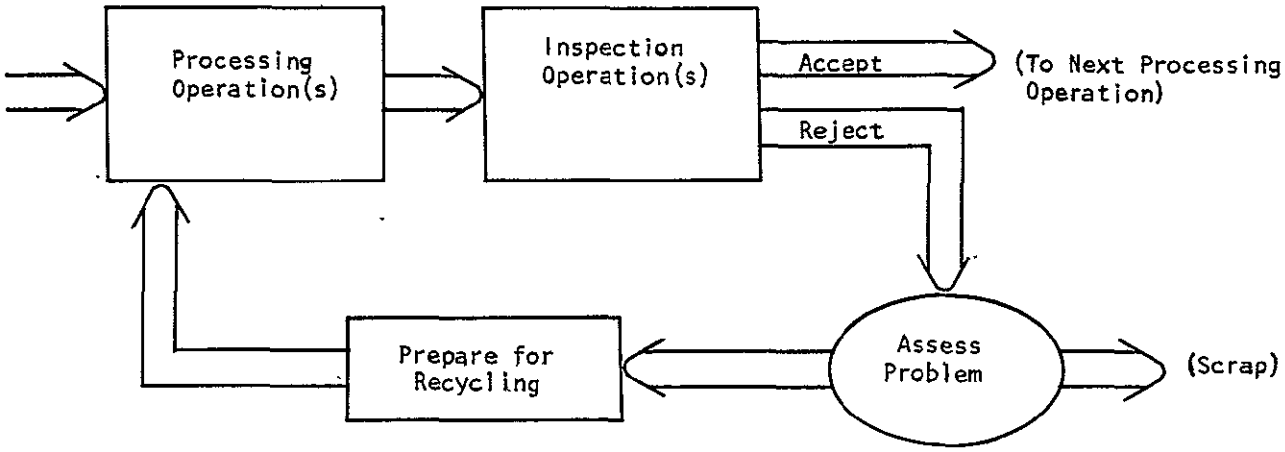

Figure A5 Illustration of Yield Concepts for Process Analysis of an Uncoupled Block.

where K_y is now the costs for finite values of b and c, scrap and recycle fallout. This expression is valid for all values of a, b, and c subject to the requirement that:

$$a + b + c = 1$$

This latter constraint is applied to maintain conservation of parts. It assures that parts are not created or lost somewhere in the cycle. Algebraic simplification of the expression for K_y and substituting the $a + b + c = 1$ constraints reduces the expression to:

$$K_y = \frac{K_i}{a},$$

which is equivalent to the straight yield concept for a single process step.

6.5.3 Compounding Yield Factors

Determination of total part cost in the presence of yield factors less than 100% may now be accomplished by a compounding process. It must be recognized that more than one part must be processed by the first operation to provide a good part to enter the next processing cycle. This effect then is compounded over all cycles to arrive at the actual total part cost. The expression for the accumulated cost, K_{ac}, of N blocks of process/inspection sequences in a complete manufacturing operation is given by:

$$K_{ac} + \sum_{i=1}^{N} \frac{K_i}{\prod_{j=1}^{i} Y_j} \tag{63}$$

where: N = total number of sequences involved

K_i = process costs for the i^{th} step

Y_j = yield factor for the i^{th} step

Solution of the above expression gives not only the total manufacturing costs for various Y_j factors, but it also defines how many parts must enter the first step to produce one acceptable part for shipment to the customer. Intermediate solutions of this expression describe the "accumulated value" of the part at some point in the process.

Another method of cost definition is the "added value concept." The added value imparted to a part by a particular operation sequence is determined by subtracting the accumulated cost of the i-1 block from the i^{th} block. This concept places emphasis on the impact of fallout associated with the last few process steps in the overall manufacturing sequence owing to the relatively high value of parts at this point.

"Actual process/inspection block costs" can also be defined when yield factors are introduced by considering the number of parts that must be produced in a particular block to result in production of one acceptable part for shipment to the customer. The costs are defined by the equation:

$$K_{yi} = \frac{K_i}{\prod_{j=i}^{N} Y_j} \tag{64}$$

where: K_{yi} = actual cost of the i^{th} block

K_i = process cost of i^{th} block at 100% yield

Y_j = overall yield factor for the i^{th} block

N = total number of blocks in the sequence

The actual block cost method puts heavy weight on the initial blocks of the manufacturing sequence because these preliminary operations must be performed more times than the last few steps. This effect is magnified if the absolute block costs of the first sequence are much larger than the last ones.

The preceding discussion was provided as an aid in evaluating the relative cost data of Volume I, for both methods of cost summation produce the same total per part cost.

6.6 Glossary of Terms

The various terms utilized in the cost model equations have been summarized in this section for convenience. Some basic standardization of these terms has been improved as an interpretive aid. The following general definitions have been made:

C = raw material costs, $/unit quantity

K = manufacturing costs for one process step, $

m = number of machines tended per operator

n = number of blades in a batch process

t = process cycle times, minutes

W = weight

Various subscripts were used to differentiate between specific terms and to identify the particular process described by the variable.

C_{brs}	ODSS	weight cost of ODSS bar stock
C_c	FRS	core cost
C_{cer}	DS/DSE	mold ceramic cost by weight
C_f	FRS	cost of fibers by weight
C_{ic}	ODSS	internal coating cost
C_m	DS/DSE	cost of master melt by weight
C_{mcl}	ODSS	MCL batch cost
C_{pw}	FRS	weight cost of powder
C_w	DS/DSE	wax cost by weight
C_{273}	Coating	internal coating cost
C_{68}	Coating	external coating cost
f_{fl}	Machine & Finish	roughing infeed per pass
f_{g2}	Machine & Finish	finish infeed per pass
K_{asf}	FRS	assemble airfoil
K_{br}	ODSS	braze

K_c	DS/DSE	casting
K_{cim}	Machine & Finish	cast in matrix
K_{cl}	DS/DSE	cluster parts cost
K_{ct}	ODSS	cooling tube
K_g	DS/DSE	grind costs
K_{ecm}	ODSS	electro-chemical machining
K_{fa}	Final Accept.	final acceptance inspection
K_{fai}	DS/DSE	final acceptance
K_{fi}	FRS	fibers
K_{fia}	ODSS	final fabrication inspection
K_{fg}	ODSS	forging
K_{fm}	FRS	fabricate monotapes
K_{fop}	Machine & Finish	finishing operations
K_{fp}	ODSS	fabricate preform
K_{gr}	Machine & Finish	root grinding
K_{gs}	Machine & Finish	serration grinding
K_{ht}	DS/DSE	heat treat
K_{iam}	FRS	post machining inspection
K_{ic}	ODSS	internal coating
K_{idc}	Coating	internal coating
K_{odc}	Coating	external coating
K_{im}	FRS	material inspection
K_{imt}	FRS	monotape inspection
K_{inl}	ODSS	first inspection
K_{ins}	ODSS	inspection

K_{ip1}	DS/DSE	first in-process inspection
K_{ip2}	DS/DSE	second in-process inspection
K_{is}	FRS	sheet inspection
K_{mac}	ODSS	machining
K_{maf}	FRS	machine airfoil
K_{mat}	FRS	mat assembly
K_{mm}	DS/DSE	master melt
K_{p}	DS/DSE	pattern
K_{pb}	DS/DSE	polish and blend
K_{pfa}	Machine & Finish	final inspection
K_{pff}	Machine & Finish	final acceptance
K_{pfg}	Machine & Finish	grinding
K_{pfi1}	Machine & Finish	first post fabrication inspection
K_{pfi2}	Machine & Finish	second post fabrication inspection
K_{pm}	DS/DSE	mold preparation
k_{pow}	FRS	powder cost
K_{pp}	DS/DSE	pattern preparation
K_{rc}	DS/DSE	core removal
K_{rm}	ODSS	raw material
K_{rt}	ODSS	root exert
K_{s}	FRS	powder sheet
K_{stp}	FRS	stamp plies
K_{tc}	Machine & Finish	thermal cycle
K_{tcg}	DS/DSE	trim casting
K_{tg}	Machine & Finish	tip grind

l	DS/DSE	withdrawal length during directional solidification
l_1	ODSS	ECM length of center cavity
l_2	ODSS	ECM depth of T/E holes
l_{gl}	Machine & Finish	roughing infeed per pass
l_s	Machine & Finish	stroke length
m_1	ODSS	ECM cavity machines per operator
m_2	ODSS	ECM T/E holes machines per operator
m_f	DS/DSE	number of casting furnaces per operator
m_p	FRS	number of presses per operator
n_1	ODSS	ECM cavity batch number
n_2	ODSS	number of blades on ECM T/E hole batch
n_a	ODSS	number in an autoclave batch
n_b	FRS	blades per acid tank
n_{bct}	ODSS	batch number for a braze furnace cycle
n_{brt}	ODSS	batch number for furnace cycle
n_{bp}	FRS	blades per press
n_c	DS/DSE	cluster number
n_f	DS/DSE	furnace batch number
n_{fb}	Machine & Finish	furnace batch number
n_g	Machine & Finish	grinding batch size
n_m	FRS	number of blades in a press
n_{mcl}	ODSS	MCL batch size
n_{mt}	FRS	number of blades from a monotape
n_{opb}	FRS	tanks per operator
n_{pb}	FRS	number of blades obtained from a metal powder batch

n_{rb}	FRS	blades in a roll batch
n_{rm}	FRS	batch size when mat is rolled
n_s	Machine & Finish	number of sparkout strokes
t_{aab}	ODSS	assemble and braze
t_{aac}	Machine & Finish	atomic absorption check
t_{aam}	ODSS	airflow inspection after machining
t_{acf}	DS/DSE	final alloy inspection
t_{act}	ODSS	assemble cooling tube
t_{ai}	FRS	airflow inspection
t_{aip}	FRS	assemble in monotape press
t_{amp}	DS/DSE	assemble mold parts
t_{as}	Machine & Finish	acid soak
t_{asr}	Machine & Finish	acid soak and rinse
t_b	FRS	core removal time
t_{baf}	FRS	blend airfoil
t_{bct}	ODSS	braze cooling tube
t_{bdt}	DS/DSE	blend
t_{be}	ODSS	blend
t_{bld}	FRS	blend and mix metal powder
t_{blt}	DS/DSE	blast blade
t_{brt}	ODSS	braze root
t_{but}	DS/DSE	buff
t_{cat}	DS/DSE	check alloy type
t_{cbt}	Machine & Finish	core blast
t_{cd}	ODSS	coat preform with lubricant
t_{cf}	FRS	cut foil

t_{cfl}	Machine & Finish	core flush
t_{gs}	DS/DSE	check grain size
t_{ci}	DS/DSE	cluster inspection
t_{cim}	Machine & Finish	cast in matrix
t_{cln}	Machine & Finish	clean blade
t_{cmt}	FRS	cut mats
t_{cof}	ODSS	clean
t_{cop}	ODSS	cut off preform
t_{cot}	DS/DSE	cut off from cluster and trim
t_{crc}	DS/DSE	core removal check
t_{cs}	FRS	coat separators
t_{ct}	DS/DSE	casting without withdrawal
t_{ctf}	DS/DSE	furnace cycle for heat treat
t_{cut}	FRS	cut fiber cloth into sheets
t_{cve}	Machine & Finish	visual core examination
t_{cwt}	DS/DSE	check wall thickness
t_{d}	Machine & Finish	dress
t_{dam}	ODSS	dimensions after machining
t_{db}	Machine & Finish	degrease blade
t_{dbr}	ODSS	deburr
t_{dc}	DS/DSE	dress cluster
t_{dcc}	DS/DSE	dehumidify ceramic cluster
t_{dd}	DS/DSE	dip and dry during investment
t_{dfb}	ODSS	degrease for braze
t_{di}	FRS	dimensional inspection

t_{dic}	DS/DSE	dress and inspect cores
t_{dif}	ODSS	dimensional inspection of forging
t_{dim}	DS/DSE	dimensional inspection
t_{dit}	FRS	density inspection time
t_{dmf}	DS/DSE	final dimensional inspection
t_{dp}	ODSS	deburr preform
t_{ds}	ODSS	descale
t_{emp}	FRS	evacuate press for monotapes
t_{ep}	FRS	evacuate press for airfoil
t_{es}	FRS	etch separators
t_{ets}	FRS	etch separators for monotapes
t_{fad}	FRS	final dimension inspection of airfoil
t_{fav}	Final Acceptance	visual inspection
t_{fci}	DS/DSE	fire, clean, and inspect mold
t_{ggr}	DS/DSE	grind gating root
t_{ggt}	DS/DSE	grind gating tip
t_{gtl}	ODSS	grind airfoil to length
t_{hf}	ODSS	heat and forge
t_{hp}	FRS	hot press
t_{hpt}	FRS	monotape hot press cycle
t_{ic}	ODSS	coat inspection cost
t_{ida}	Machine & Finish	core alloy inspection
t_{iec}	Coating	external coating inspection
t_{iic}	Coating	internal coating inspection
t_{ifp}	DS/DSE	inspect final pattern

t_{imp}	DS/DSE	inject mold parts
t_{ip}	DS/DSE	inject pattern
t_{l}	Machine & Finish	load
t_{lp}	FRS	load press
t_{ltp}	FRS	load monotape press
t_{mar}	Final Acceptance	markings
t_{mat}	FRS	mat assembly
t_{mfr}	ODSS	machine for root
t_{mop}	Machine & Finish	marking operations
t_{mt}	FRS	monotape thickness inspection
t_{mw}	DS/DSE	melt out wax from mold
t_{pa}	FRS	polish airfoil
t_{paa}	Machine & Finish	AA inspection
t_{pfa}	Machine & Finish	airflow inspection
t_{pfcb}	Machine & Finish	corner break
t_{pfd}	Machine & Finish	degrease
t_{pfw}	Machine & Finish	wash
t_{prs}	FRS	press time
t_{pt}	DS/DSE	polish time
t_{pvi}	Machine & Finish	core & T/E visual inspection
t_{rc}	DS/DSE	autoclave cycle
t_{rdi}	Machine & Finish	root dimensional inspection
t_{rfp}	FRS	remove monotapes from press
t_{rft}	FRS	roll fibers for collimation
t_{rm}	FRS	remove monotapes

t_{rol}	FRS	roll time
t_{rmv}	Machine & Finish	root and matrix visual inspection
t_{sal}	FRS	stack and load press
t_{sl}	Machine & Finish	slurry
t_{sp}	Final Acceptance	shot peen
t_{st}	FRS	stamp plies from monotapes
t_{stf}	DS/DSE	snag T/E flash
t_{tfa}	ODSS	airflow check
t_{tfd}	ODSS	dimensional inspection
t_{thi}	FRS	thickness inspection
t_{up}	FRS	unload press
t_{vam}	FRS	visual inspection
t_{vc}	Machine & Finish	visual check
t_{vcf}	DS/DSE	final visual core examination
t_{ve}	ODSS	visual inspection
t_{vet}	ODSS	visual examination
t_{vis}	DS/DSE	visual inspection
t_{vmi}	FRS	visual inspection of mat
t_{wtf}	DS/DSE	final wall thickness inspection
t_{xam}	FRS	X-ray airfoil
t_{xrm}	FRS	X-ray monotape
t_{zb}	Machine & Finish	zyglo blade
t_{zy}	DS/DSE	zyglo inspection
T_{c1}	Machine & Finish	total roughing depth of cut
T_{c2}	Machine & Finish	total finish depth of cut

v	DS/DSE	withdrawal velocity
v_1	ODSS	ECM electrode velocity for cavity machining
v_2	ODSS	ECM electrode velocity for T/E hole machining
V	Machine & Finish	table velocity
W_{cer}	DS/DSE	ceramic weight
W_f	FRS	fiber batch weight
W_m	DS/DSE	metal weight in a pour
W_{mr}	DS/DSE	revert metal weight
W_p	ODSS	preform weight
W_{pb}	FRS	powder batch weight
W_{wmp}	DS/DSE	wax weight for mold parts
W_{wp}	DS/DSE	wax pattern weight
W_{wr}	DS/DSE	wax revert weight

Distribution List for CR 135203 DATE--> 10/03/77
1 copy except as noted in parentheses

NASA Headquarters
600 Independence Ave., SW
Washington, DC 20546
Attn RWM/J. Gangler

NASA Lewis Research Center
21000 Brookpark Road
Cleveland, OH 44135
Attn R.L. Dreshfield
MS 105-1

NASA Lewis Research Center
21000 Brookpark Road
Cleveland, OH 44135
Attn C.P. Blankenship
MS 105-1
(6 copies)

NASA Lewis Research Center
21000 Brookpark Road
Cleveland, OH 44135
Attn N.T. Saunders
MS 501-2

NASA Lewis Research Center
21000 Brookpark Road
Cleveland, OH 44135
Attn R. L. Davies
MS 106-1

NASA Lewis Research Center
21000 Brookpark Road
Cleveland, OH 44135
Attn C. M. Scheuermann
MS 49-3

NASA Lewis Research Center
21000 Brookpark Road
Cleveland, OH 44135
Attn H.B. Probst, MS 49-3

NASA Lewis Research Center
21000 Brookpark Road
Cleveland, OH 44135
Attn S.J. Grisaffe
MS 49-3

NASA Lewis Research Center
21000 Brookpark Road
Cleveland, OH 44135
Attn S.G. Young, MS 49-3

NASA Lewis Research Center
21000 Brookpark Road
Cleveland, OH 44135
Attn R.A. Signorelli
MS 106-1

NASA Lewis Research Center
21000 Brookpark Road
Cleveland, OH 44135
Attn R.A. Rudey, MS 60-4

NASA Lewis Research Center
21000 Brookpark Road
Cleveland, OH 44135
Attn M&S Division File
MS 49-1

18

NASA Lewis Research Center
21000 Brookpark Road
Cleveland, OH 44135
Attn Contracts Section B
MS 500-313

NASA Lewis Research Center
21000 Brookpark Road
Cleveland, OH 44135
Attn Tech Utilization
MS 3-19

NASA Lewis Research Center
21000 Brookpark Road
Cleveland, OH 44135
Attn Library, MS 60-3
(2 copies)

NASA Lewis Research Center
21000 Brookpark Road
Cleveland, OH 44135
Attn AFSC Liason Office
MS 501-3

NASA Lewis Research Center
21000 Brookpark Road
Cleveland, OH 44135
Attn AAMRDL, MS 77-5

NASA Lewis Research Center
21000 Brookpark Road
Cleveland, OH 44135
Attn Report Control
MS 5-5

NASA Langley Rsch Center
Langley Field, VA 23365
Attn Library

NASA MSFC
Huntsville
AL 35812
Attn W. B. McPherson

U.S. Air Force
Wright-Patterson AFB
OH 45433
Attn AFML/LLM N. Geyer

U.S. Air Force
Wright-Patterson AFB
OH 45433
Attn AFAPL/TBP T. Norbut

U.S. Air Force
Wright-Patterson AFB
OH 45433
Attn AFML/LTM H. Johnson

U.S. Air Force
Wright-Patterson AFB
OH 45433
Attn AFAPL/TBP L.J. Obery

U.S. Air Force
Wright-Patterson AFB
OH 45433
Attn AFML/LL L. Hjelm

U.S. Air Force
Wright-Patterson AFB
OH 45433
Attn AFML/LAM Library

U.S. Air Force
Wright-Patterson AFB
OH 45433
Attn ASD/YZES W. Crow

NASA STIF
Attn Accessioning Dep't
P.O. Box 8757
Balt-Wash Int'nat Airport
Maryland 21240
(10 copies)

DATE--> 10/03/77

Eustis Directorate
U.S. Army Air Mobility
R & D Laboratory
Fort Eustis, VA 23604
Attn J. Lane SAVDL-EU-TAP

AVSCOM
P.O. Box 209
St. Louis, MO 63166
Attn W. McClane
DRSAV-EQA

Army Materials &
Mechanics Research Center
Watertown, MA 02172
Attn Library

Navy Department
Naval Air Systems Command
Washington, D.C. 20361
Attn I. Machlin
Air-52031B

Naval Air Dev. Center
Warminster, PA 18974
Attn M. K. Thomas

Research & Technology Div.
NAPTC
Trenton, NJ 08628
Attn J. Glatz

Navy Department
Naval Ship R&D Center
Annapolis, MD 21402
Attn G. A. Wacker 2812

ERDA
Washington, DC 20545
Attn J. Neal

AiResearch Mfg. Company
P.O. Box 5217
Phoenix, AZ 85010
Attn C. Corrigan 93-12

AiResearch Mfg. Company
P.O. Box 5217
Phoenix, AZ 85010
Attn R. Kirby

AiResearch Mfg. Company
P.O. Box 5217
Phoenix, AZ 85010
Attn M. Duffy

AVCO Lycoming Div.
550 S. Main St.
Stratford, CT 06497
Attn B. Goldblatt

Curtiss-Wright Corp.
1 Passaic St
Wood Ridge, NJ 07075
NJ 07075
Attn J. Mogul

Detroit Diesel Allison
P.O. Box 894
Indianapolis, ID 46206
Attn M. Herman

General Electric Co.
Gas Turb Prod. Div.
Schenectady, NY 12345
Attn C. Sims, Bldg 53

General Electric Co.
Gas Turb Prod. Div.
Schenectady, NY 12345
Attn F. D. Lordi, Bldg 53

General Electric Co.
Material and Processing
Technology Laboratory
Evandale, OH 45415
Attn E. Bamberger

General Electric Co.
Material and Processing
Technology Laboratory
Evandale, OH 45415
Attn D. Arnold

General Electric Co.
AEG/GED
1000 Western Ave.
Lynn, MA 01910
Attn J. Hsia

General Electric Co.
336 S. Woodward Ave., SE
Albuquerque, NM 87102
Attn R.W. Smashey

General Electric Co.
Corporate R+D Center
P. O. Box 8
Schenectady, NY 12301
Attn Library

Pratt and Whitney Aircraft
Commercial Products
400 Main St.
East Hartford, CT 06108
Attn R. A. Sprague

Pratt and Whitney Aircraft
Commercial Products
400 Main St.
East Hartford, CT 06108
Attn A. Hauser

Pratt and Whitney Aircraft
Manufacturing Div.
400 Main St.
East Hartford, CT 06108
Attn J. Zubeckis

Pratt and Whitney Aircraft
Box 2691
West Palm Beach
FL 33402
Attn J. Moore

Solar
Div of Int. Harvester
P.O. Box 80966
San Diego, CA 92138
Attn A. Stetson

Teledyne CAE
Mat. Dev. and Manuf. Engr
PO Box 6971
Toledo, OH 43612
Attn R. Beck

Williams Research
2280 W. Maple
Walled Lake, MI 48081
Attn Wm. P. Schimell

DATE--> 10/03/77

Battelle Memorial Inst
505 King Ave.
Columbus, OH 43210
Attn P.W. Boulger

Boeing - Wichita Div.
Wichita, KS 67210
Attn Wm. F. Schmidt
org. 75930 Propulsion

Cameron Iron Works
P. O. Box 1212
Houston, TX 77001
Attn Library

Cannon-Muskegon Corp.
P.O. Box 506
Muskegon, MI 49443
Attn R. Schwer

Certified Alloys Products
3245 Cherry Ave.
Long Beach, CA 90807
Attn M. Woulds

Climax Molybdenum Co.
P.O. Box 1568
Ann Arbor, MI 48106
Attn C. Clark

Douglas Aircraft Co.
McDonnell Douglas Corp
3855 Lakewood Blvd.
Long Beach, CA 90846
Attn Library

Ford Motor Company
Metallurgical Dept.
P.O. Box 2053
Dearborn, MI 48121
Attn C. Feltner

General Motors Corp.
Technical Center
Warren, MI 48090
Attn E. Reynolds

Grumman Aerospace Corp.
Bethpage, NY 11714
Attn C. Hoelzer plant 5

Howmet Corporation
Technical Center
699 Benston Rd.
Whitehall, MI 49461
Attn W. Freeman

Howmet Corporation
Austenal Division
Dover, NJ 07801
Attn F. Jaeger

83

Howmet Corporation
Turbine Components Div.
Dover, NJ 07801
Attn E. Carozza

IIT Research Institute
10 West 35th Street
Chicago, IL 60616
Attn M. A. Howes

International Nickel Corp
Sterling Forest
Suffern, NY 10901
Attn Library

Jetshapes, Inc.
Rockleigh Industrial Park
Rockleigh, NJ 07647
Attn R. J. Quigg

MCIC
Battelle Memorial Inst.
505 King Ave.
Columbus, OH 43201

Rocketdyne Division
Rockwell International
6633 Canoga Ave.
Canoga Park, CA 91304
Attn T.G. McNamara

Rockwell International
Columbus Aircraft Div.
P. O. Box 125901
Columbus, OH 43209
Attn J. T. DeLany

Rockwell International
Science Center
Thousand Oaks, CA 91360
Attn N. Paton

Special Metals, Inc.
Middle Settlement Road
New Hartford
New York 13413
Attn C. Carlson

Stellite Division
Cabot Corporation
1020 West Park Ave.
Kokomo, IN 46901
Attn S. T. Wlodek

Teledyne Allvac
P. O. Box 759
Monroe, NC 28110
Attn F. Elliott

United Airlines - SFOEG
San Francisco Airport
CA 94128
Attn J. K. Goodwine

United Tech Rsch Center
East Hartford, CT 06108
Attn Library

Vought Corp.
P.O. Box 5907
Dallas TX 75222
Attn Library
2-50370/TL 7-67

Vought Missiles and Space
3221 No. Armistead Ave.
Hampton, VA 23366
Attn C.W. Pearce

Westinghouse R + D Center
Beulah Rd.
Pittsburgh, PA 15236
Attn D. Moon

DATE--> 10/03/77

Westinghouse Electric Co.
P.O. Box 10864
Pittsburgh, PA 15236
Attn R. L. Ammon

118